



# An Exceptionally Preserved Terrestrial Record of LIP Effects on Plants in the Carnian (Upper Triassic) Amber-Bearing Section of the Dolomites, Italy

Guido Roghi<sup>1</sup>, Piero Gianolla<sup>2</sup>, Evelyn Kustatscher<sup>3,4,5</sup>, Alexander R. Schmidt<sup>6</sup> and Leyla J. Seyfullah<sup>7\*</sup>

<sup>1</sup>Institute of Geosciences and Earth Resources (IGG-CNR), Padova, Italy, <sup>2</sup>Department of Physics and Earth Sciences, University of Ferrara, Ferrara, Italy, <sup>3</sup>Museum of Nature South Tyrol, Bolzano, Italy, <sup>4</sup>Department für Geo- und Umweltwissenschaften, Paläontologie und Geobiologie, Ludwig-Maximilians-Universität, Munich, Germany, <sup>5</sup>Bayerische Staatssammlung für Paläontologie und Geologie, Munich, Germany, <sup>6</sup>Department of Geobiology, University of Göttingen, Göttingen, Germany, <sup>7</sup>Department of Palaeontology, University of Vienna, Vienna, Austria

## OPEN ACCESS

### Edited by:

Sara Callegaro,  
University of Oslo, Norway

### Reviewed by:

Daoliang Chu,  
China University of Geosciences  
Wuhan, China  
Grzegorz Pacyna,  
Jagiellonian University, Poland

### \*Correspondence:

Leyla J. Seyfullah  
leyla.seyfullah@univie.ac.at

### Specialty section:

This article was submitted to  
Paleontology,  
a section of the journal  
Frontiers in Earth Science

**Received:** 20 March 2022

**Accepted:** 01 June 2022

**Published:** 11 July 2022

### Citation:

Roghi G, Gianolla P, Kustatscher E, Schmidt AR and Seyfullah LJ (2022) An Exceptionally Preserved Terrestrial Record of LIP Effects on Plants in the Carnian (Upper Triassic) Amber-Bearing Section of the Dolomites, Italy. *Front. Earth Sci.* 10:900586. doi: 10.3389/feart.2022.900586

The Carnian Pluvial Episode (CPE) has been recognized as a time of plant radiations and originations, likely related to observed swift changes from xerophytic to more hygrophytic floras. This suggests that the increasing humidity causally resulting from LIP volcanism was the trigger for these changes in the terrestrial realm. Understanding the cause and effects of the CPE on the plant realm, requires study of well-preserved floras that are precisely aligned with the CPE. We therefore focus on the best age-constrained section within the CPE for the terrestrial to marginal marine environment to understand the floristic composition at the early CPE. This is found in the Dolomites, Italy, and is remarkable for the preservation of the oldest fossiliferous amber found in the rock record. An integrated study of palynomorphs and macro-remains related to the conifer families of the fossil resin bearing level brings together the floral components from this section. This observed mixture of different taxa of extinct and modern conifer families underlines firmly the effects of the LIP-induced CPE on the evolution and radiation of conifers.

**Keywords:** Carnian Pluvial Episode (CPE), palynomorphs, plant fossils, amber, paleoenvironmental reconstruction, conifer evolution and radiation

## INTRODUCTION

The Triassic is generally considered as having hothouse conditions with no polar icecaps. The presence of the supercontinent Pangaea over the paleoequator led to a drier continental interior despite a strong monsoonal system (Tanner, 2018). This allowed two main floristic provinces to develop, one in the Northern Hemisphere (Laurussia) and the other in the Southern Hemisphere (Gondwana). During the Late Triassic (237–201 Ma), Pangaea started to fragment, and the floras show increased provincialism in addition to compositional shifts in reaction to major climatic pulses (Buratti and Cirilli, 2007; Preto et al., 2010; Kustatscher et al., 2018; Tanner, 2018). Palynofloras divide Gondwana in to two sub-provinces: the cooler and perhaps more humid *Falcisporites* (Umkomasiales) dominated Ipswich Sub-province found between 90° and 40°S paleolatitude, and the warmer and more diverse Onslow Sub-province found around 45° to 20°S paleolatitude (Dolby



**FIGURE 1** | Pangaeian floristic subprovinces during the Late Triassic (modified from Kustatscher et al., 2018). The red area marks the likely paleogeographic position of the Wrangellia LIP volcanism, linked to the CPE. Thicker line indicates the divide between the Laurussian and Gondwanan areas. Star indicates the paleogeographic position of the Dolomites area, the question mark indicates area with no data.

and Balme, 1976; Césari and Colombi, 2013; Kustatscher et al., 2018). In Laurussia, seven floral sub-provinces have been recognized, linked to the more varied regional environmental and climate conditions (Kustatscher et al., 2018; **Figure 1**).

During the Carnian (237–227 Ma, early Late Triassic), profound changes are observed in both the marine and terrestrial realms. These changes have been linked to a global climate upheaval termed the Carnian Pluvial Episode (CPE) that occurred around 234 to 232 Ma (Simms and Ruffell, 1989; Simms and Ruffell, 1990; Simms et al., 1995; Dal Corso et al., 2020; Colombi et al., 2021). The increased hydrological cycle and weathering resulted in increased siliciclastic input into the basins (Rigo et al., 2007; Dal Corso et al., 2015; Dal Corso et al., 2020).

The isotopic analyses of these multiple siliciclastic occurrences in the Tethys area define the presence of global negative carbon isotopic excursions (NCIEs) linked to large, pulsed injections of isotopically depleted  $\text{CO}_2$ . The carbon isotopic perturbations suggest that the CPE was caused by LIP volcanism repeatedly injecting vast amounts of  $^{13}\text{C}$  carbon depleted carbon dioxide into the Carnian atmosphere-ocean system warming the world, with the Wrangellia LIP thought to be the major source for these carbon injections (Dal Corso et al., 2012; Dal Corso et al., 2015; Sun et al., 2016; Miller et al., 2017; Dal Corso et al., 2018; Dal Corso et al., 2020; Lu et al., 2021; Mazaheri-Johari et al., 2021; Tomimatsu et al., 2020; Dal Corso et al., 2022). Palynological analyzes of the levels with the NCIEs allow the definition of discrete humid impulses based on the dominance of hygrophytic elements in the palyno-assemblages (Roghi et al., 2010; Mueller et al., 2016a; Mueller et al., 2016b; Baranyi et al., 2019). The Heiligkreuz and Travenanzes formations of the Dolomites (Italy) were the key in linking the NCIEs and the increased siliciclastic occurrences with the signals observed from the plants (e.g., Preto and Hinnov, 2003; Breda et al., 2009; Roghi et al., 2010; Stefani et al., 2010; Dal Corso et al., 2015; Dal Corso et al., 2018). The warmer, wetter climate enhanced the hydrological cycle, resulting in large quantities of terrigenous material and nutrients entering

the sea basins. The duration of the entire CPE event is estimated to be around 1.2 Myr (Zhang et al., 2015; Miller et al., 2017; Bernardi et al., 2018; Lu et al., 2021).

This time of significantly increased global rainfall (Preto et al., 2010) even resulted in substantial coal deposits in geographically distinct areas i.e., in Laurussia (Austria, Svalbard, Sweden, China) and in Gondwana (Australia, South Africa), as summarized by Retallack et al. (1996) and Ruffell et al. (2016). The CPE has been related to a major extinction event with subsequent biotic radiations, resulting from an abruptly warmed climate. Many key groups that dominate modern ecosystems appear to have undergone an explosive diversification due to the CPE leading to the “dawn of the modern world” (Dal Corso et al., 2020).

The plant fossil record is intermittent for the Late Triassic and is often only resolved to stage level, meaning that identifying within-stage floral responses such as to the CPE (late Tuvalian to Julian substages of the Carnian) is not always clear-cut (Kustatscher et al., 2018; Dal Corso et al., 2020). There are, however, clear switches to humid elements in the late early Carnian floras, with a return to floras characterized by drier elements during the late Carnian (e.g., Roghi et al., 2010; Kustatscher et al., 2018; Baranyi et al., 2019; Kustatscher et al., 2019). Also, paleosol analysis from Italy (Dolomites) and Spain highlight more humid conditions during the CPE than before and after it (Breda et al., 2009; Barrenechea et al., 2018). The CPE is thought to have led to the diversification of some key Mesozoic plant groups such as the Bennettitales, plus the origination and radiation of several modern fern and conifer families (Kustatscher et al., 2018; Dal Corso et al., 2020). Amber, fossilized plant resin, is also a distinct feature of some Carnian floras (Roghi et al., 2006a; Schmidt et al., 2006; Schmidt et al., 2012; Seyfullah et al., 2018a; Seyfullah et al., 2018b). Although trace amounts of amber are found in earth history from the Carboniferous onwards, these are microscopic amounts from within the plant tissues (Seyfullah et al., 2018a; Seyfullah et al., 2018b). The first appearance of significant amounts of amber in the fossil record is during the Carnian (Seyfullah et al., 2018a;

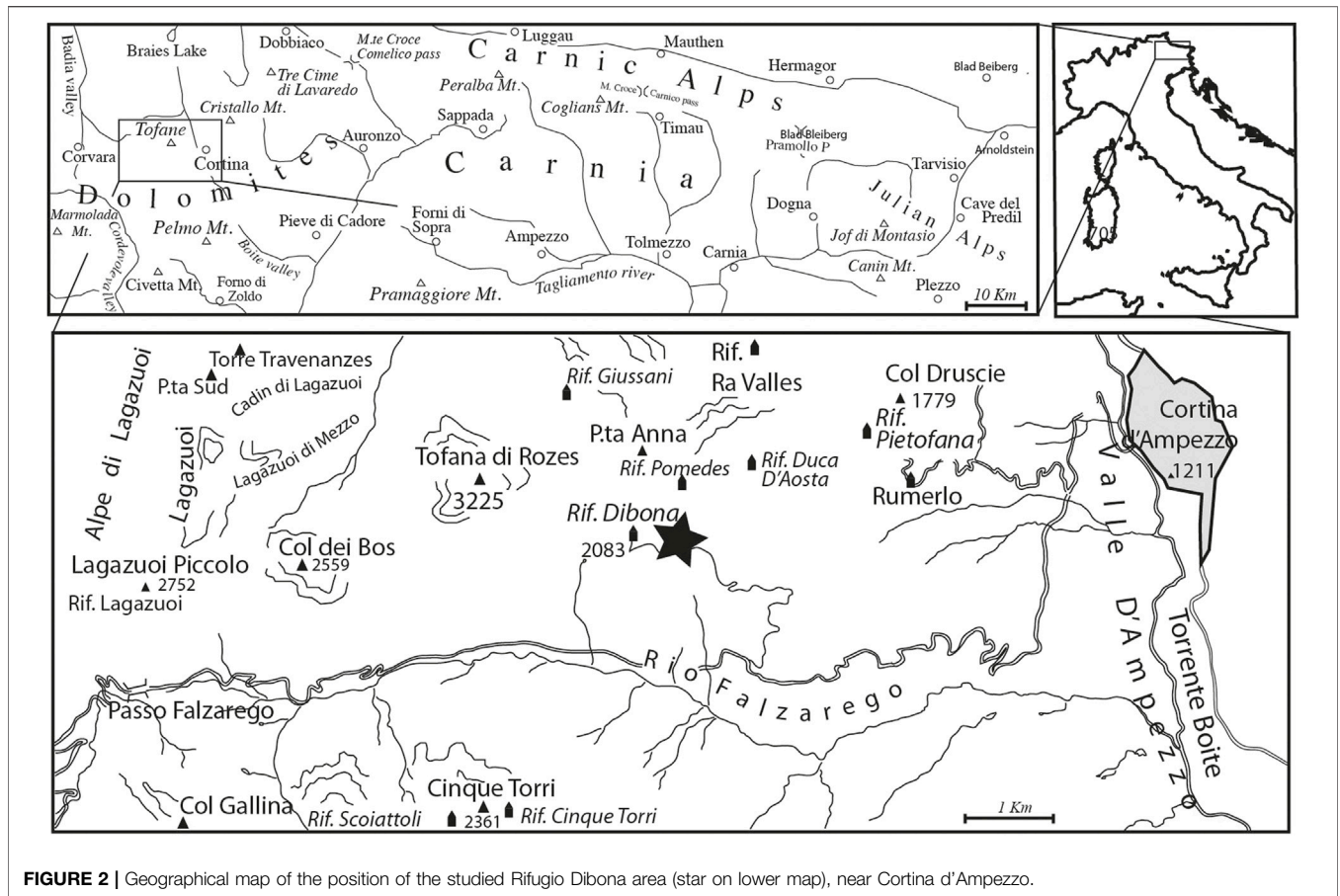


FIGURE 2 | Geographical map of the position of the studied Rifugio Dibona area (star on lower map), near Cortina d'Ampezzo.

Seyfullah et al., 2018b). It is hypothesized that the resin outpourings preserved as amber deposits indicate environmental stresses on the terrestrial environment (Gianolla et al., 1998a; Roghi et al., 2006a; Seyfullah et al., 2018a; Seyfullah et al., 2018b).

Carnian amber has yielded the oldest inclusions in amber in the fossil record. Although the search for inclusions also in other Triassic ambers is promising (Stilwell et al., 2020), a substantial amount is only found from the Heiligkreuz Fm., in the Italian Dolomites, so far. Also, here a large volume of small amber droplets is preserved in paleosols (Preto and Hinnov, 2003; Schmidt et al., 2006; Breda et al., 2009; Schmidt et al., 2012). The entrapped organisms span plant remains, including pollen and spores, invertebrate remains and microorganisms, giving us a rare insight into the terrestrial realm during the CPE and telling us at a very fine scale the incredibly local interaction of the plants and the surrounding biota (Schmidt et al., 2006; Schmidt et al., 2012; Sidorchuk et al., 2015). This amber deposit is the largest by volume of amber of all the Carnian-aged deposits (Seyfullah et al., 2018a). To understand the responses of the plants to the CPE we focus on the best age-constrained section exposing the CPE: the Rifugio Dibona section near the town of Cortina d'Ampezzo, Dolomites, Italy (Figure 2). The section of the Rifugio Dibona is one of the most continuous, complete, and best studied outcrops of the Heiligkreuz Formation, the lithostratigraphic unit that

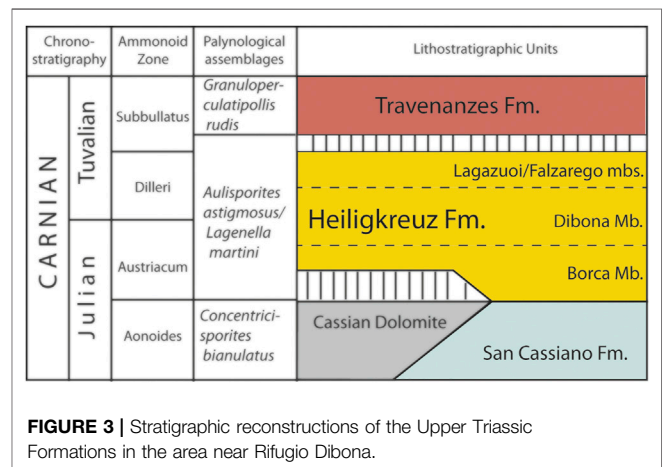


FIGURE 3 | Stratigraphic reconstructions of the Upper Triassic Formations in the area near Rifugio Dibona.

records the CPE in the Dolomites (De Zanche et al., 1993; Gianolla et al., 1998b; Preto and Hinnov, 2003; Breda et al., 2009; Maron et al., 2017) and can be easily correlated with other sections of the same unit in the Dolomites (Neri et al., 2007).

In addition to the amber-rich paleosols, macro- and microfossil remains have also been recovered from the Heiligkreuz Fm. at the Rifugio Dibona section (Roghi et al., 2006a; Dal Corso et al., 2011). Here we focus on these three

botanical indicators: Plant macrofossils, palynomorphs and amber, to show the effects on the flora during the CPE. Particularly interesting are the gymnospermous plant remains since those have a reduced taphonomic and collecting bias compared to the sporing plants (e.g., Nowak et al., 2018).

## GEOLOGICAL INFORMATION

In the upper Carnian of the Dolomites, the passage from the carbonate-siliciclastic sediments of the heteropic San Cassiano Formation/Cassian Dolomite, to the Heiligkreuz Formation, is well documented. (see Dürrenstein Fm. in Bosellini, 1984; De Zanche et al., 1993; Gianolla et al., 1998a; Gianolla et al., 1998b; Keim and Brandner, 2001; Keim et al., 2001; Neri et al., 2007; Gattolin et al., 2015) (**Figure 3**).

The lower portion of the Heiligkreuz Fm., also known as Borca Mb. (Neri et al., 2007; Breda et al., 2009; Gattolin et al., 2015; Dal Corso et al., 2018) consists of terrigenous-carbonate facies with well-stratified dolomitic limestones, arenaceous dolomites and hybrid arenites with frequent pelitic intervals. At the base of the Heiligkreuz Fm. there are biostromes with diversified colonial corals, stromatoporoids and sponges, often well preserved in aragonite both in the Alpe di Specie/Seelandalpe and Dibona areas (Scherer, 1977; Russo et al., 1991; Senowbari-Daryan et al., 2001; Neri et al., 2007; Gianolla et al., 2018). The corals that make up these structures, which will never form the edges of large platforms, are of the modern type (Stanley, 2003).

The upper portion of the Borca Mb. is frequently made up of ooliths and peritidal stromatolitic dolomites covered by polycyclic paleosols levels typical of humid climates (Preto and Hinnov, 2003; Breda et al., 2009). In the middle part of the Heiligkreuz Fm. there is a transgressive unit rich in silicoclastics: Calcarenites and biocalcarenes, sometimes oolitic, which make up the Dibona Mb. (Bosellini et al., 1982; Preto and Hinnov, 2003; Neri et al., 2007) and which upwards become nodular hemipelagic limestones. In those lower siliciclastic facies and in the pelitic-clayey levels of paleosols there is a large quantity of fossil resin together with abundant plant remains (Gianolla et al., 1998b; Roghi et al., 2006a).

The top of the Heiligkreuz Fm., called the Lagazuoi Mb., consists of shallow water bioclastic carbonates, which pass laterally to terrigenous sediments (Falzarego Mb. in Neri et al., 2007). On the top there is a discordant surface consisting of dolomitic breccias (Keim and Brandner, 2001). With the deposition of the Lagazuoi Mb., the paleotopography of the area is definitively flattened. Subsequently there are transgressive alluvial and muddy facies of Tuvalian age (Travenanzes Fm.) which are superimposed by a Heiligkreuz Fm. discordance and are in turn covered by carbonate peritidal cycles of the Hauptdolomit/Dolomia Principale (Breda and Preto, 2011).

Near the base of the Heiligkreuz Fm. the *Aulisporites astigmus* and *Lagenella martini* sporomorph association was identified, and the presence of the ammonoids *Austrotrachyceras* sp. and *Sirenites senticosus* confirm the base of the Julian 2 stage

(Breda et al., 2009). In the middle part of the Heiligkreuz Fm. the sporomorph *Lagenella martini* Assemblage (Roghi et al., 2010) defines the Julian 2–Tuvalian 1 age (Roghi et al., 2010; Maron et al., 2017). In the upper part of the Heiligkreuz Fm., together with the ammonoids *Shastites* cfr. *pilari* and cfr. *Jovites* sp., the conodonts *Paragondolella noah* and *Metapolygnathus praecommunisti*, confirm a Tuvalian 1 age (Breda et al., 2009; Maron et al., 2017). The Julian-Tuvalian boundary is thus located in the upper part of Heiligkreuz Fm., where the Tuvalian ammonoids are found, and is marked by a NCIE. The section with the amber-bearing paleosols exposed at the Rifugio Dibona area has been dated to a Julian 2–Tuvalian 1 (late early–early late Carnian; *Austrotrachyceras austriacum*–*Tropites dilleri* ammonoid zones) of the Heiligkreuz Fm. using ammonoids, conodonts and sporomorphs (Gianolla et al., 1998b; Gianolla et al., 2003; De Zanche et al., 2000; Neri et al., 2007; Roghi et al., 2010; Dal Corso et al., 2015).

The succeeding Travenanzes Fm. is assigned to the Tuvalian 2 by the presence of the *Granuloperculatipollis rudis* assemblage, which is calibrated in the Julian Alps to Tuvalian 2–3 (Roghi, 2004). The Julian 2–Tuvalian 1 interval, well identified in the Heiligkreuz Fm.–Travenanzes Fm. succession, by ammonoids, conodonts and palynomorphs, and is characterized by strong variations in the isotope ratio of organic carbon organized in different events often associated with macroscopic siliciclastic inputs (Dal Corso et al., 2015; Dal Corso et al., 2018). In particular, in the Heiligkreuz Fm., exposed right at the Rifugio Dibona (**Figure 4**), various NCIEs have been identified both with carbon isotopes of the dispersed organic matter, biomarkers and isotopes of the organic carbon of wood present along the entire section. The first of these excursions allow us to define the onset of the CPE whereas two other NCIE events along the sections, and always within the CPE, were also identified. The last shift is present at the base of the Travenanzes Fm. Since the carbon isotopic variation affects both marine and terrestrial fossil molecules, this isotopic variation has its origin in changes of atmospheric, and consequently, terrestrial and marine environments (Dal Corso et al., 2012).

## MATERIALS AND METHODS

### Plant Macrofossils

Plant macrofossils are composed mainly of impressions and compressions, with occasional small fragments of charcoal; 29 specimens have been collected and deposited at the Museum of Nature South Tyrol, where they are stored by consecutive numbers prefixed by the acronym “PAL”. Specimens were photographed with a Canon EOS D550 digital camera and measured using the free software ImageJ64® (National Institute of Health, Bethesda, MD).

### Paleosols

Paleosol beds (**Figure 4**) were recognized and followed along different points of the Rifugio Dibona section. The thin (few cm thick) paleosols are usually found lying over karstified surfaces

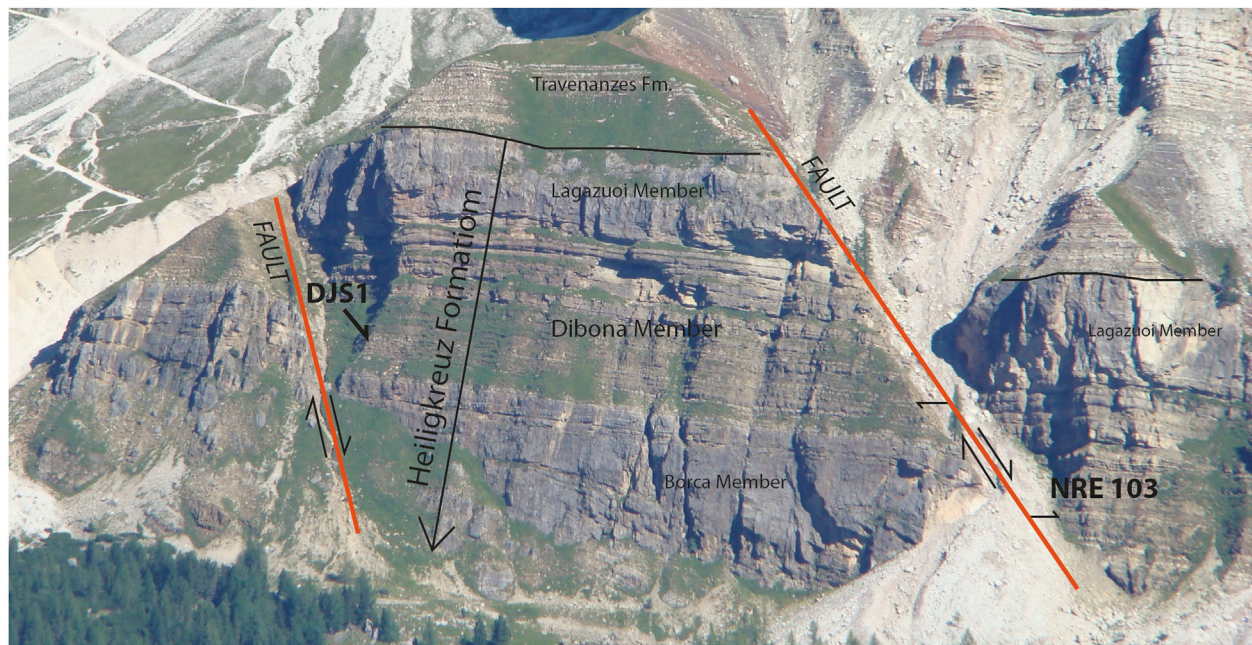


**FIGURE 4** | The main outcrops of the Heiligkreuz Fm. exposed at the Refugio Dibona section and the position of the levels of the palynological samples DJS 1 and NRE 103. The paleosol rich in amber crops out at level NRE 103. The distance between the two sampling sites is approximately 250 m, for scale.

(Preto and Hinnov, 2003; Gattolin et al., 2013) with a spodic (Fe-alluvial) horizon under an overlying histic (rich in organic matter) horizon. Breda et al. (2009) used these features to infer that the soil developed in a humid climate during the CPE. One of the paleosols was sampled and subsets were processed for palynological and amber studies (see below).

## Pollen

In order to best identify the diversity of plant communities during the CPE, the paleosol level containing a large amount of fossil resin was sampled for the palynological analyses at two different positions of the Rifugio Dibona section, at a distance of about 250 m, respectively DJS 1 and NRE 103 (Figure 4). Both qualitative and quantitative analyses (two slides for each sample) were performed showing a high similarity in qualitative and quantitative composition on the microassemblages. Specimens were photographed with a DFC300 camera at a Leica DMLB microscope. The studied material is housed at the Institute of Geosciences and Earth Resources (IGG-CNR), Padova. Additional palynomorphs are present as amber inclusions and are housed at the Museum of Geology and Paleontology, University of Padova.

## Amber

The amber droplets were elutriated from the paleosol in water and any adhered plant remains removed. The clean droplets were placed on hollowed glass microscope slides (Menzel Inc.) immersed in water, covered by a glass coverslip and screened for inclusions under a Carl Zeiss AxioScope A1 compound microscope as described by Schmidt et al. (2012).

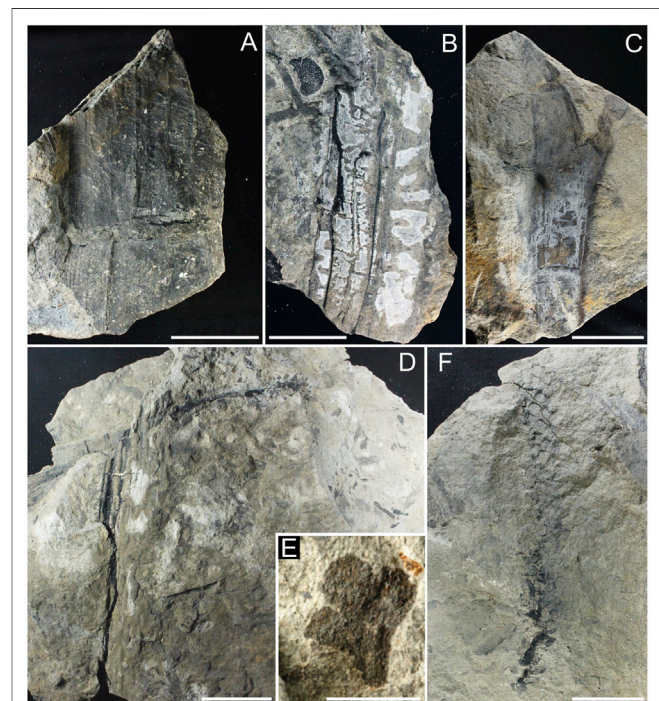
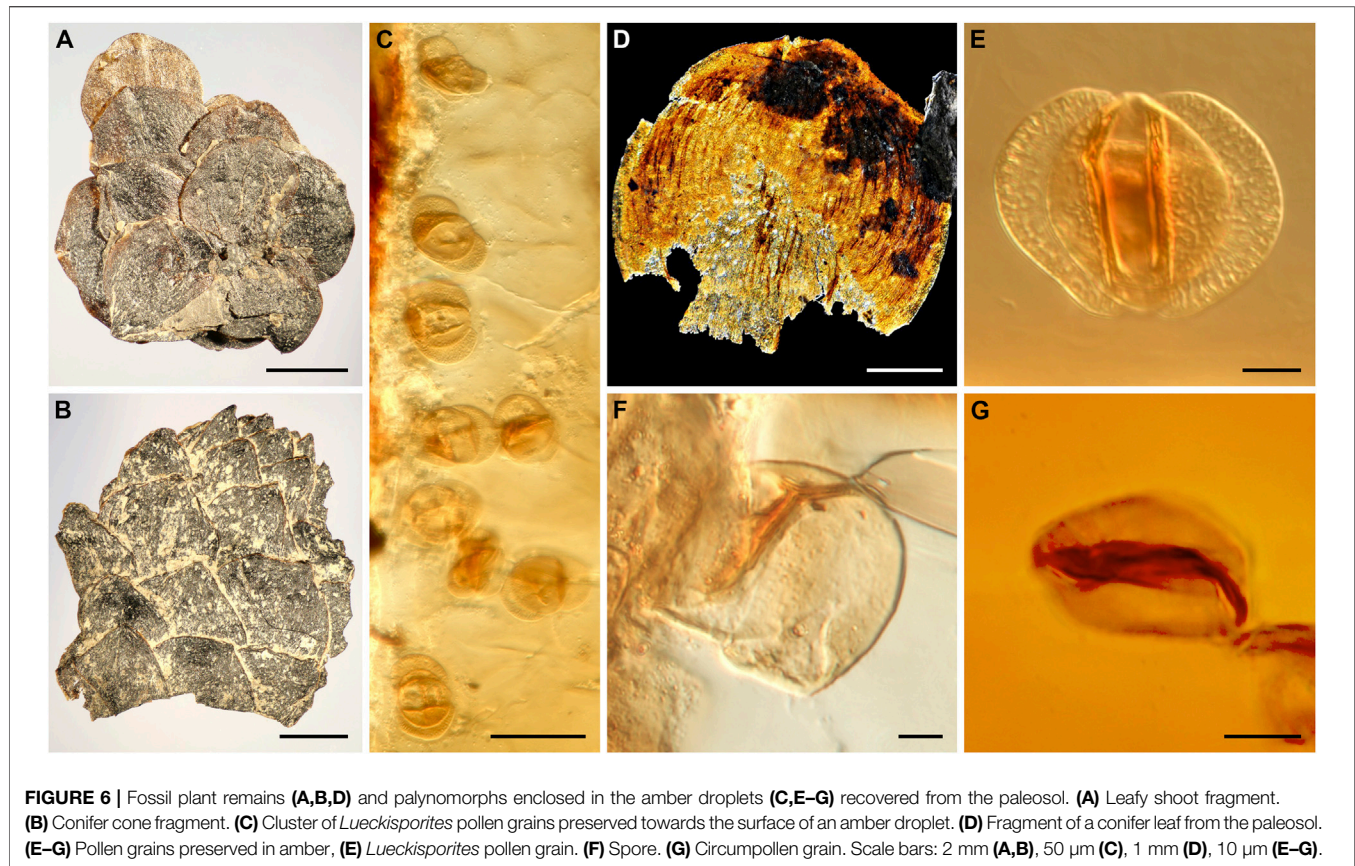


**FIGURE 5** | Plant macrofossils of the Heiligkreuz Fm. (A) Sphenophyte, PAL 4121 NRE103 72; (B) Sphenophyte, PAL 4100 NRE103 52; (C) Undetermined stem, PAL 4107 NRE103 60; (D) *Voltzia* sp., PAL 4107 NRE103 60; (E) Trilobate leaf; (F) *Voltzia* sp., PAL 4111 NRE103 61. Scale bars: 5 cm (A–D,F); 1 cm (E).



The millimetre-sized amber droplets containing palynomorphs and plant remains were embedded in a high-grade ‘glass conservation’ epoxy (EpoTek 301-2, Epoxy Technology) and subsequently ground and polished to bring the inclusions close to the surface of the preparation, for enhanced imaging (refer to Sadowski et al., 2021, for protocols).

Prepared specimens were placed on a glass microscope slide with a drop of water applied to the upper surface of the amber, covered with a glass coverslip. This reduces light scattering from fine surface scratches and improves optical resolution. Specimens were photographed with a Carl Zeiss AxioScope A1 compound microscope, using up to 640 magnification and differential interference contrast (DIC) illumination.

## RESULTS

### Plants of the Heiligkreuz Fm.: Macrofossils

The macrofossil plant assemblage is composed mainly by sphenophyte stem fragments, stem, shoot, leaves and cone fragments of conifers, seeds, a putative axis fragment of a lycophyte, some less well-defined stem fragments that occasionally bifurcate, fragments of charcoal, and amber dispersed among and/or attached to the top of the plant remains (Figure 5).

The sphenophyte stem fragments are up to 300 mm long and 150 mm wide. Most fossils are composed by impressions or compressions of the stems with visible impressions of the vascular bundles, often also with desiccation cracks perpendicular to the axes. Internal casts of the stems, diaphragm fragments and rhizome fragments with attachment of the arising subaerial axis are preserved. Elongate structures, up to 230 mm long and 13 mm wide, with a thick central vein/midvein could also belong to this group, as smaller axes.

The conifer fragments are generally small and often represented by up to 200 mm long and 35 mm wide stem fragments of the *Endolepis* type characterized by a knotty surface of the stem. Conifer shoots are up to 160 mm long and 20 mm wide, partly defoliated. Leaves are falcate in lateral view, 7–13 mm long and 1.8–2.5 mm wide with a rounded apex. In frontal view they are lanceolate, the leaf scar impression is almost rhombohedral in shape with a diameter of 6.8–7 mm. One trilobate ovuliferous scale is also preserved; it is less than 10 mm long and wide.

Smaller plant remains include a dispersed seed of up to 16 mm diameter with a slightly pointed apex. The outer layer, preserved only as carbonate material, is about 1 mm thick. A very small plant fragment is composed of bifurcating axis fragments, up to 30 mm long and 2–2.5 mm wide. The single leaves are ovate to scale-like, less 1–1.5 mm long and 1 mm wide, and closely

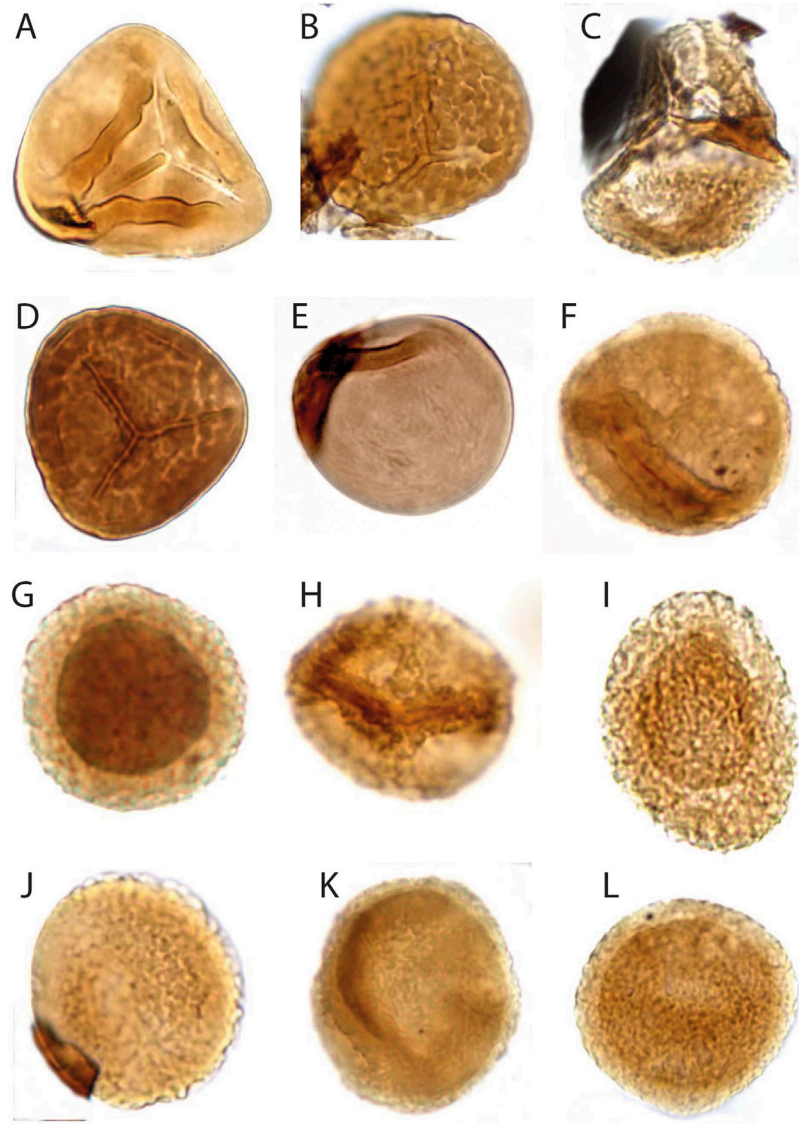


**FIGURE 7** | Palynomorphs of the Heiligkreuz Fm., part I. **(A)** *Concavisporites toralis*; slide DJS1A III; O29/3; 57  $\mu\text{m}$  height. **(B)** *Convolutispora* sp. A; slide DJS1A III; O54/1; 46,4  $\mu\text{m}$  diameter. **(C)** *Kraeuselisporites* sp.; NRE103A IV; L24; 52  $\mu\text{m}$  height. **(D)** *Convolutispora* sp. Ind.; DJS1A III; S53/2; 43  $\mu\text{m}$  diameter. **(E)** *Leschikisporites aduncus*; NRE103B III, H32; 35  $\mu\text{m}$  diameter. **(F)** *Aratrisporites scabratus*; DJS1A III; R52/2; 34  $\mu\text{m}$  diameter. **(G)** *Vallasporites ignacii*; DJS1A III, L33/4; 28,8  $\mu\text{m}$  diameter. **(H)** *Vallasporites ignacii*; DJS1A III, N29/2; 32  $\mu\text{m}$  diameter. **(I)** *Patinasporites* cf. *P. densus*; DJS1A II, J43/1; 40  $\mu\text{m}$  height. **(J)** *Haberkornia parva*; DJS1A III, O51; 32  $\mu\text{m}$  diameter. **(K)** *Enzonalasporites vigens*; DJS1A III, N24; 40  $\mu\text{m}$  diameter. **(L)** *Enzonalasporites vigens*; DJS1A II, J43/1; 43  $\mu\text{m}$  diameter.

imbricated. This fragment could represent a lycophyte-type of plant such as *Selaginellites*.

### Plants of the Heiligkreuz Fm.: Mesofossils

The paleosol yielded a rich assemblage of dispersed leaves and small conifer shoot and cone fragments with exceptionally well-preserved cuticles (Figures 6A,B,D). The leaf fragments are broadly lanceolate with a rounded apex, up to 2–2.5 mm long and 3 mm wide. They are partly macerated, showing the rows of the stomata. The base and attachment area of the leaves is

irregular, suggesting that the leaves were not naturally shed but defoliated during transport and deposited in the paleosol. The general shape and dimension of the leaves as well as the cuticles suggest that they belong to the conifers.

### Plants of the Heiligkreuz Fm.: Palynomorphs

The palynological analyses of the samples taken at levels DJS 1 and NRE 103 yielded a rich and diverse assemblage of spores, pollen,

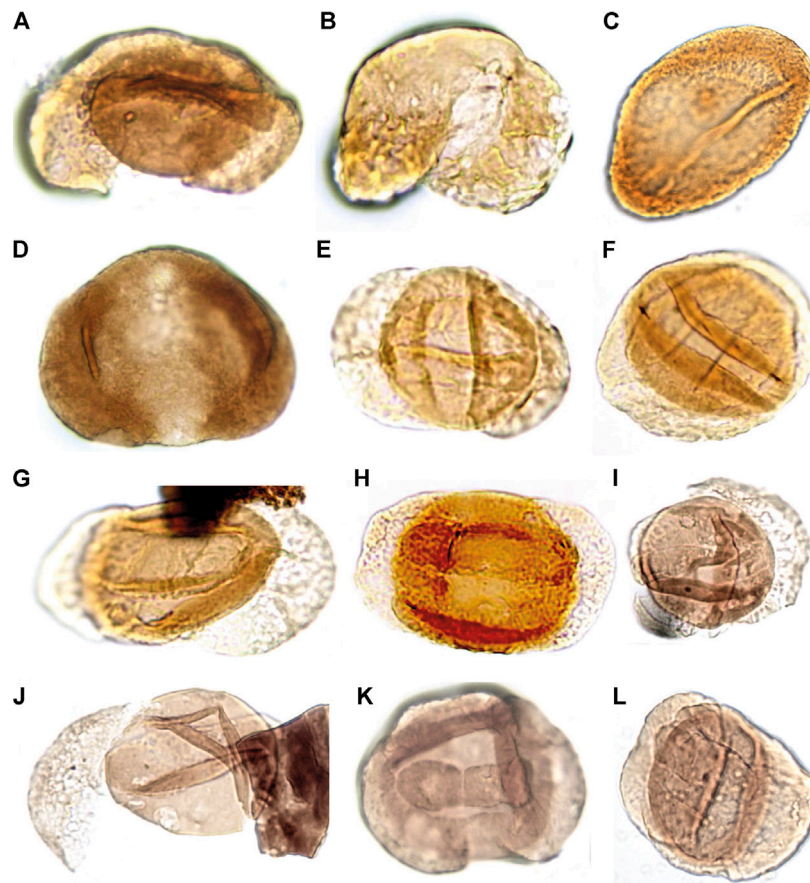


**FIGURE 8** | Palynomorphs of the Heiligkreuz Fm., part II. **(A)** *Samaropollenites speciosus*; DJS1A I, J38/1, 55  $\mu\text{m}$  width. **(B)** *Abietinaepollenites* sp.; DJS1A I, T45/3, 46  $\mu\text{m}$  width. **(C)** *Chordasporites* sp.; NRE103B II, S48, 83  $\mu\text{m}$  width. **(D)** *Klausipollenites schaubegeri*; DJS1A I, Q29/2, 72  $\mu\text{m}$  width. **(E)** *Lunatisporites acutus*; DJS1A III, H45/2, 46  $\mu\text{m}$  width. **(F)** *Lueckisporites junior*; NRE103B I, N40/3, 52  $\mu\text{m}$  width. **(G)** *Taeniato* sp. 1; NRE103B III, R33/2, 48  $\mu\text{m}$  height. **(H)** *Lueckisporites junior*; DJS1A I, J52/4, 72  $\mu\text{m}$  length. **(I)** *Samaropollenites* sp.; DJS1A II, L33, 37  $\mu\text{m}$  corpus diameter. **(J)** *Samaropollenites* sp.; DJS1A II, L33, 36  $\mu\text{m}$  corpus diameter. **(K)** *Taeniato* sp. 2, DJS1A I, G36/4, 50  $\mu\text{m}$  width. **(L)** *Lunatisporites acutus*; NRE103B III, S35/3, 51  $\mu\text{m}$  height.

cuticle fragments and amber. The most diverse are the pollen grains with about 30 different forms, whereas the spores are less diverse with eight different types. The spores are represented by trilete laevigate (e.g., *Concavisporites*, *Calamospora*), trilete ornamented (e.g., *Osmundacidites*, *Convolutispora*) and monolete cavate (e.g., *Aratrisporites*) forms. The pollen grains include a variety of bisaccate taeniate (e.g., *Lunatisporites*, *Lueckisporites*), bisaccate non-taeniate (e.g., *Klausipollenites*, *Triadispora*), monosaccate (e.g., *Enzonalasporites*, *Patinasporites*), circumpollen (e.g., *Duplicisporites*, *Paracirculina*), and alete forms (e.g., *Araucariacites*) (Figures 7–9).

The two samples DJS 1 and NRE 103 are relatively uniform in their quantitative composition (Figure 10). The sporomorph assemblage of sample DJS 1 is dominated by bisaccate taeniate pollen grains (69%). Second in order of abundance are the monosaccate pollen grains (13%), trilete spores (5%), bisaccate alete pollen grains (5%), and circumpollen (6%). Rare are alete pollen grains (1%) and marine sporomorphs (1%), whereas bisaccate trilete pollen grains are missing. The sporomorphs of

the sample NRE 103 are dominated by bisaccate taeniate pollen grains (61%). Second in order of abundance are the trilete spores (13%), circumpollen (12%), and monosaccate pollen grains (7%). More rare are the bisaccate trilete (3%), bisaccate alete, and alete pollen grains, and marine sporomorphs (each 2%).

If the botanical affinities of the sporomorphs are considered, the conifer pollen grains are the most represented and diverse group (19/30 genera). For most conifer pollen grains, with the exception of *Klausipollenites* and perhaps *Lunatisporites*, an affinity with conifers has been suggested or proven by *in situ* findings (Table 1). Most of the conifer pollen are related to the Majonicaceae (4/19 genera), Cheirolepidiaceae (4/19 genera), and Voltziaceae (3/19 genera). However, also the families Podocarpaceae (*Samaropollenites*), Araucariaceae (*Araucariacites*), Pinaceae (*Abietinaepollenites*) are represented in the palynological record. The monosaccate pollen grains are assigned to the Voltziales but without any detailed botanical affinity since the so far only *in situ* record is that of the putative

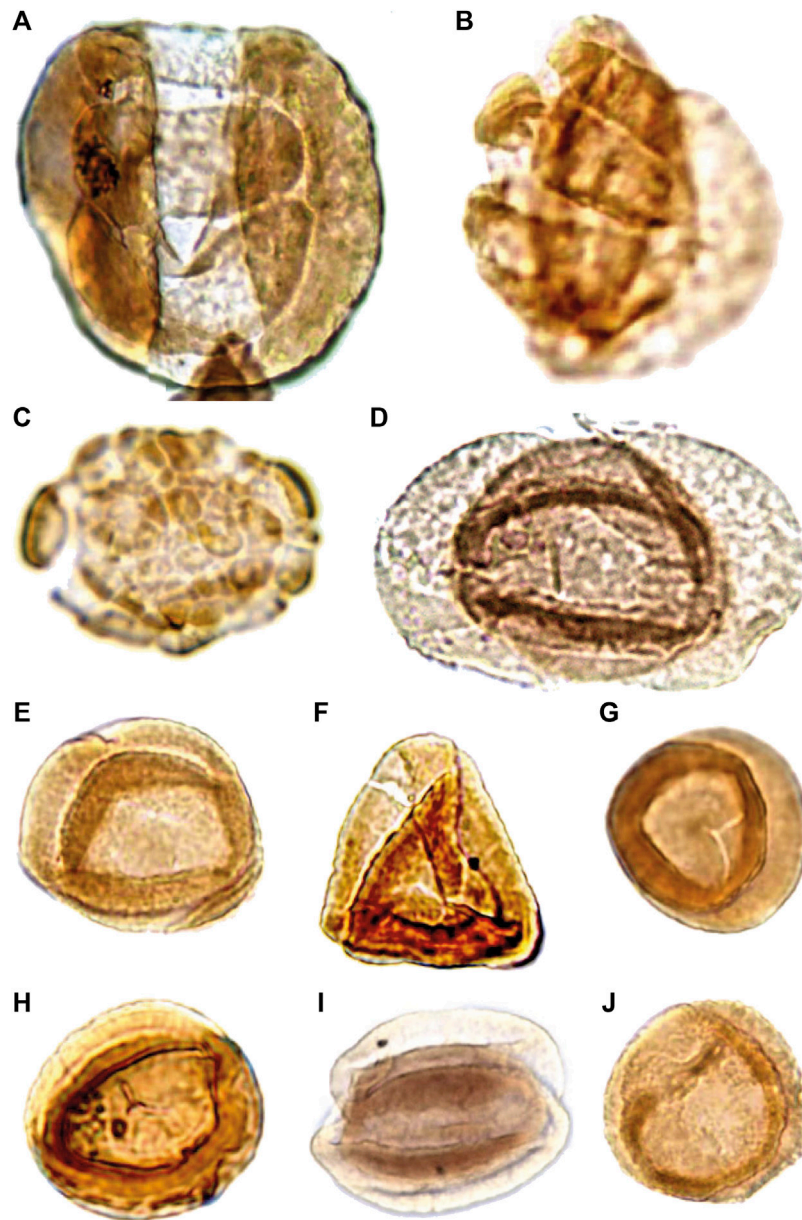
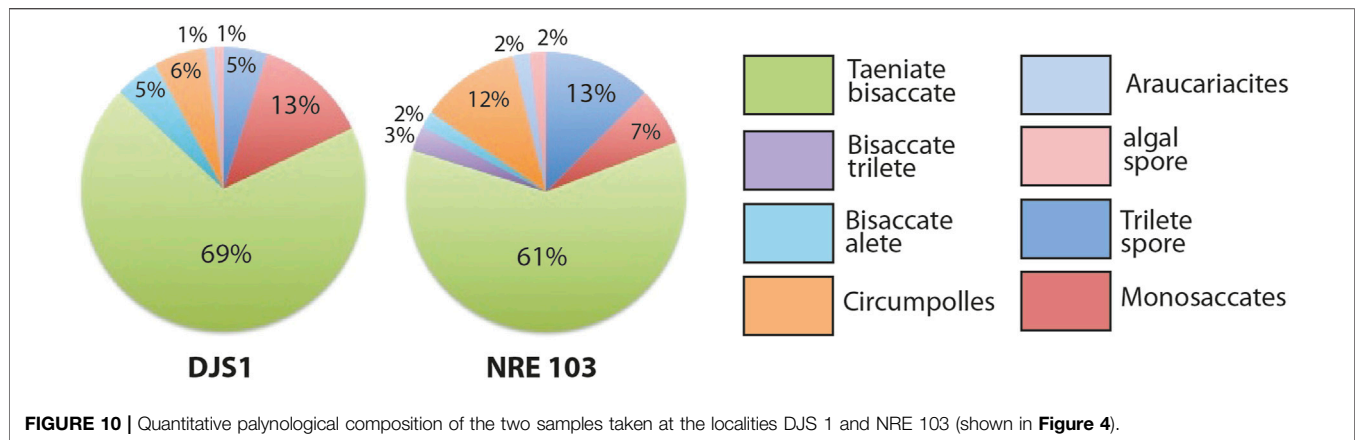


**FIGURE 9** | Palynomorphs of the Heiligkreuz Fm., part III. **(A)** *Infernopollenites sulcatus*; DJS1A I, G34/1; 50  $\mu\text{m}$  height. **(B)** *Infernopollenites* sp.; DJS1A I, F47/3; 48  $\mu\text{m}$  height. **(C)** *Camerosporites secatus*; DJS1A I, N24, 27  $\mu\text{m}$  diameter. **(D)** *Lueckisporites* cf. *L. virkkiae*; NRE103B III, J27, 51  $\mu\text{m}$  width. **(E)** *Duplicisporites granulatus*; DJS1A II, O28/1, 32  $\mu\text{m}$  diameter. **(F)** *Duplicisporites granulatus*; NRE103A IV, X38, 35  $\mu\text{m}$  height. **(G)** *Duplicisporites granulatus*; DJS1A III, H42/2, 32  $\mu\text{m}$  diameter. **(H)** *Paracirculina maljawkinae*; NRE103B I, D37/4, 29  $\mu\text{m}$  diameter. **(I)** *Duplicisporites granulatus*; NRE103B III, S34/4, 36  $\mu\text{m}$  diameter. **(J)** *Duplicisporites granulatus*; DJS1A II, K36, 32  $\mu\text{m}$  diameter.

voltzialean *Patokaea silesiaca* (Pacyna et al., 2017). Among the spores dominate those of the lycophytes (4/10 genera) and the ferns (4/10 genera).

Observing the ecological distribution of the potential parent plants (Table 1), many taxa belong to plants typical of coastal environments (11/30 genera), which include conifers of the families Cheirolepidiaceae, Araucariaceae and Majonicaceae, as well as lycophytes (Table 1). Also well represented are elements

typical of the lowland (9/30). This environment is mostly represented by hygrophytic elements (5/10 genera) that include representatives of the ferns and lycophytes, as well as more xerophytic elements (4/10 genera) that include seed ferns, putative conifers and/or cycadophytes. Less diverse are the hinterland elements (5/30 genera), which are mostly represented by Voltziaceae and Pinaceae conifers. The most humid areas as inferred from the palynology are interpreted as



having standing fresh water (5/30 genera) and were occupied by sphenophytes, Podocarpaceae (conifers) and Schizaeaceae (ferns).

Considering the relative abundance of the sporomorphs it becomes evident that the most abundant group is that of the hinterland elements, plants that live in environments above the permanent ground water level. This is why they are often indicated as “upland” elements, although this term can be misleading and here does not refer to any sporomorphs originating from areas with significant elevation, only to those from drier environments. They reach 69% in sample DJS 1 and about 64% in NRE 103. The coastal elements are second in order of abundance, with 15–24% in DJS 1 and 21% in NRE 103. Rarer are the lowland dry elements (2–8%) and wet elements typical of standing water bodies (4–8% in DJS 1 and 13% in NRE 103).

## Amber

Carnian ambers are the oldest in the fossil record with inclusions. The most abundant and diverse inclusions are from the thousands of the usually 2–6 mm sized amber droplets, discovered in the paleosols exposed at the Rifugio Dibona section (**Figure 11A**). The droplets comprise 2–5% by volume of the paleosol which is equivalent to several thousand droplets per square metre, underlining the phenomenal amber richness of the paleosols (Schmidt et al., 2006; Schmidt et al., 2012; Seyfullah et al., 2018a). The amber source plant for these droplets has been previously identified as members of the Cheirolepidiaceae (e.g., Schmidt et al., 2012).

The amber droplets are famous for its inclusions of microorganisms and small arthropods. From the amber droplets have been described perfectly preserved unicellular organisms such as algal and fungal spores, bacteria, ciliate protozoans and testate amoebae (Schmidt et al., 2006), a nematoceran fly and highly specialized phytophagous mites (Schmidt et al., 2012). The mites are four-legged and represented by four distinct morphologies. They were assigned to the new superfamily Triasacaroidea, which is probably a sister group to the Eriophyoidea (extant gall mites) (Sidorchuk et al., 2015). It was also possible to show that the fossil resin was also preserved as blebs inside the conifer leaves (**Figure 11B**). During

the Late Triassic the insects developed herbivorous modes similar to the modern ones, at least at the level of leaf piercing and sucking, and chewing causing evident signs of irritation (Labandeira, 2006). Examples of this chewing damage is also observed in the dispersed plant cuticles found in the Rifugio Dibona paleosol discussed above.

However also pollen and spores were found entrapped in the amber (**Figures 6C,E–G**). The preservation is three-dimensional permitting a comparison with dispersed pollen grains extracted from the samples NRE 103 and DJS 1. Most of the amber-preserved pollen grains are bisaccate (**Figures 6C,E**), whereas spores (**Figure 6F**) and circumpollen grains (**Figure 6G**) are rare. An exceptional group of eight bisaccate pollen grains inside the amber (**Figure 6C**) belongs all to the genus *Lueckisporites*, and appear to be mature grains.

The occurrence of several very similar pollen grains of *Lueckisporites* close to the edge of the amber in a three-dimensional state excludes a previous notion that similar grains found dispersed in the sediment could be reworked from the Permian (Balme, 1979; Utting, 2004). Pollen grains of the *Lueckisporites*-type were only found *in situ* in Permian Majonicaceae conifer cones so far (e.g., Clement-Westerhof, 1974). The presence of Majonicaceae-type of conifers has been already proposed based on a similar cuticle structure of conifer shoot fragments from the Carnian of Dogna (Roghi et al., 2006b). The presence of genuine *Lueckisporites* pollen in the Triassic has been demonstrated lately also by the presence of *in situ* pollen in Anisian conifer cones (Forte et al<sup>1</sup>). Our new findings demonstrate that Majonicaceae-type of conifers were an inherent part of the Triassic floras at least until the Carnian in the low latitudes in the peri-Tethyan areas.

<sup>1</sup>Forte, G., Kustatscher, E., Nowak, H., Van Konijnenburg-Van Cittert, J. H. A. Conifer Cone and Dwarf Shoot Diversity in the Anisian (Middle Triassic) of Kühwiesenkopf/Monte Prà Della Vacca (Dolomites, NE Italy). *Int. J. Pl. Sc.* in revision.

**TABLE 1** | The palynoflora from the paleosols exposed at the Rifugio Dibona, with inferred ecological preferences SEG, Sporomorph Eco Group; CO, Coastal; HL, Hinterland; LD, Dry Lowland; RI, River; LW, Wet Lowland.

Pollen/Spore	Botanical affinity	Ecology	SEG
<i>Araucariacites</i>	Conifer, Araucariaceae (Balme, 1995)	Xerophyte	CO
<i>Abietineaepollenites</i>	Conifer, Pinaceae (Zhang et al., 2021)	Xerophyte	HL
<i>Brachysaccus</i>	Conifer of uncertain affinity (Baranyi et al., 2019)	Xerophyte	LD
<i>Camerosporites</i>	Conifers, Cheirolepidiaceae (Baranyi et al., 2019)	Xerophyte	CO
<i>Chordasporites</i>	Conifers, perhaps Voltziaceae (Balme, 1995; Zhang et al., 2021)	Xerophyte	HL
<i>Duplicisporites</i>	Conifers, Cheirolepidiaceae (Baranyi et al., 2019)	Xerophyte	CO
<i>Enzonalasporites</i>	Conifers, Voltziales (Pacyna et al., 2017)	Intermediate	CO
<i>Haberkornia</i>	Conifer of uncertain affinity	Xerophyte	LD
<i>Infernopollenites</i>	Conifers, perhaps Majonicaceae (Zhang et al., 2021)	Intermediate	CO
<i>Klausipollenites</i>	Seed ferns (Franz et al., 2014)	Xerophyte	LD
<i>Lueckisporites</i>	Conifers, Majonicaceae, Voltziaceae (Clement-Westerhof, 1974; Baranyi et al., 2019)	Intermediate	CO
<i>Lunatisporites</i>	Conifers (Clement-Westerhof, 1974), seed ferns, Peltaspermales (Looy et al., 2001)	Intermediate	HL
<i>Ovalipollis</i>	Conifers, Voltziaceae (Baranyi et al., 2019), Cycadophyta (Barrón et al., 2006)	Xerophyte	LD
<i>Paracirculina</i>	Conifers, Cheirolepidiaceae (Zhang et al., 2021)	Xerophyte	CO
<i>Partitisporites</i>	Conifers, Cheirolepidiaceae (Baranyi et al., 2019)	Xerophyte	CO
<i>Patinasporites</i>	Conifers, Majonicaceae (Baranyi et al., 2019)	Intermediate	CO
<i>Quadraeculina</i>	Conifer of uncertain affinity (Barrón et al., 2006)	Xerophyte	HL
<i>Samaropollenites</i>	Conifers, Podocarpaceae (Bonis and Kürschner, 2012)	Hygrophyte	RI
<i>Triadispora</i>	Conifers, Voltziaceae, <i>in situ</i> in <i>Sertostrobus</i> , <i>Dameya</i> (Grauvogel - Stamm, 1978)	Xerophyte	HL
<i>Vallasporites</i>	Conifers, Majonicaceae (Baranyi et al., 2019)	Intermediate	CO
<i>Aratrisporites</i>	Lycophytes, <i>in situ</i> in <i>Cyclostrobus</i> , <i>Lycostrobus</i> (Helby and Martin, 1965), <i>Lepacyclotes zelleri</i> (Grauvogel - Stamm and Düringer, 1983)	Hygrophyte	CO
<i>Calamospora</i>	Sphenophytes, Equisetales, <i>in situ</i> in <i>Equisetites arenaceus</i> (Kelber and Van Konijnenburg - Van Cittert, 1998)	Hygrophyte	RI
<i>Concavisporites</i>	Ferns, Dicksoniaceae and Matoniaceae (Balme, 1995; Baranyi et al., 2019)	Hygrophyte	LW
<i>Concetricisporites</i>	Ferns of unknown botanical affinity (Kustatscher et al., 2010)	Hygrophyte	LW
<i>Convolutispora</i>	Ferns, Schizaeaceae (Barrón et al., 2006)	Hygrophyte	RI
<i>Kraeuselisporites</i>	Lycophytes, Lycopodiales (Balme, 1995)	Hygrophyte	LW
<i>Leschikisporites</i>	Lycophytes, Lycopodiales (Balme, 1995)	Hygrophyte	LW
<i>Osmundacidites</i>	Ferns, Osmundaceae (Balme, 1995)	Hygrophyte	LW
<i>Simplicisporites</i>	Lycophytes of uncertain affinity	Hygrophyte	RI
<i>Trilletes</i>	Spore of unknown botanical affinity (Kustatscher et al., 2010)	Hygrophyte	RI

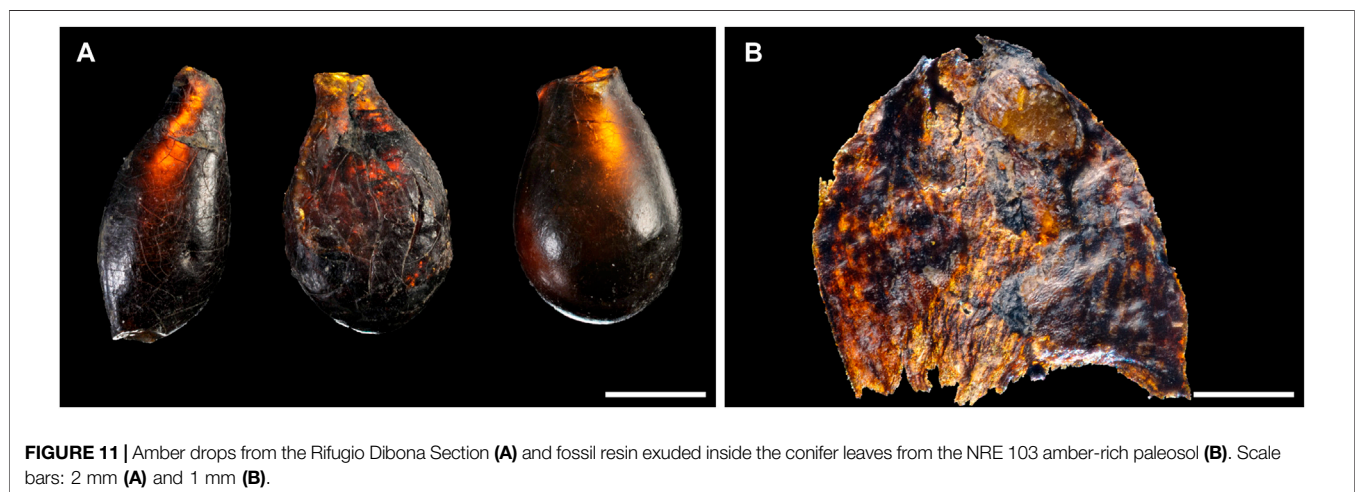


**FIGURE 11** | Amber drops from the Rifugio Dibona Section (A) and fossil resin exuded inside the conifer leaves from the NRE 103 amber-rich paleosol (B). Scale bars: 2 mm (A) and 1 mm (B).

## DISCUSSION

### The Conifers of Rifugio Dibona

Plants experienced a major evolutionary radiation during the Carnian, with the co-occurrence of a mixture of primitive (Paleozoic) and modern (Mesozoic and Cenozoic) plant

groups (Dal Corso et al., 2020) (Figure 12). One of the groups, affected more deeply by this radiation, is that of the conifers.

At the Rifugio Dibona macro-, meso-, and microplant remains show a distinct co-occurrence of a series of different conifer families. This includes the Majonicaceae represented by pollen

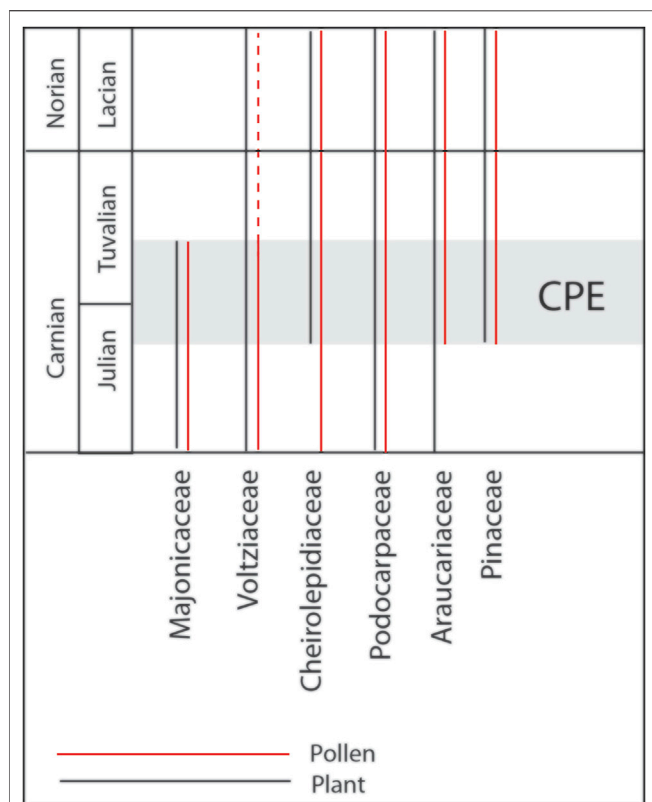


**FIGURE 12 |** Conifer family distributions along the Carnian based on macro- and micro fossil remains, see text for information.

grains dispersed in the sediment (*Lueckisporites* and *Lunatisporites*) and as inclusions in the amber. This conifer family is considered a typical element in the Southern Alps during the Permian (Clement Westerhof, 1987; Forte et al., 2017). It has been putatively described from the Carnian of the Julian Alps (Roghi et al., 2006b) and lately confidently recorded also from the early Middle Triassic (Anisian) of the Dolomites (Forte et al.<sup>1</sup>). Also, the associated monosaccate pollen grains (e.g., *Enzonalasporites* and *Patinasporites*) were probably produced by primitive voltzialean conifers, although *in situ* findings are still missing and, thus, their specific affinity is still unknown.

Typical Triassic elements are the Voltziaceae (e.g., *Triadispora*), well-represented in the microflora by bisaccate, trilete pollen grains and in the macrofossil record by small conifer shoots. Amber was not found attached to any of the voltzialean conifer shoots from Rifugio Dibona, but small amounts of amber from the Middle Triassic in the northern Dolomites demonstrated that also the Voltziaceae were resin-producers during humid climate shifts (Roghi et al., 2017; Forte et al., 2022).

<sup>1</sup>Forte, G., Kustatscher, E., Nowak, H., Van Konijnenburg-Van Cittert, J. H. A. Conifer Cone and Dwarf Shoot Diversity in the Anisian (Middle Triassic) of Kühwiesenkopf/Monte Prà Della Vacca (Dolomites, NE Italy). *Int. J. Pl. Sc.* in revision.

The circumpollen belongs to the family Cheirolepidiaceae (e.g., Roghi et al., 2006a; Kustatscher et al., 2011). The dispersed cuticles and small shoot fragments from the paleosol belong to this conifer family as well as the thousands of amber droplets that were collected from the paleosol. Summarizing, it can be said that the dominating element in the paleosol is the Cheirolepidiaceae family.

Three modern conifer families with extant representatives co-occur in the microflora of Rifugio Dibona. These are the Araucariaceae (*Araucariacites*), the Pinaceae (*Abietinaepollenites*) and the Podocarpaceae (*Samaropollenites*). This is not the oldest record of those conifer families. Several macro- and mesoremainds putatively assignable to these families were indicated already before. This includes putative araucariaceous seeds already from the Early Permian of Texas (DiMichele et al., 2001) and putative needles and cuticles of podocarpacean conifers from the Permian of Jordan (Blomenkemper et al., 2018). The so far oldest confirmed macrofossil record of Pinaceae is from the Late Jurassic (Rothwell et al., 2012). Here, a mixture of macrofossil (Voltziaceae, Majonicaceae and Cheirolepidiaceae) and pollen (Voltziaceae, Majonicaceae, Araucariaceae, Pinaceae and Podocarpaceae) is presented. This diversity of different taxa of extinct and modern conifer families strongly underlines the pronounced effect of the CPE on the evolution and radiation of the conifers.

The amber-preserved microflora (Figure 5) provides an array of paleobotanical insights. The cluster of *Lueckisporites* grains (Figure 5C) inside the amber droplet but close to its surface suggests that these grains were most likely stuck to the resin surface when the resin leaked either near the pollen cone or that the droplet oozed from the cone itself. Other findings of spores and circumpollen represent isolated grains that accidentally got stuck to the resin, perhaps transported there by wind or even animals or, for circumpollen (Figure 5), from the same tree where the pollen was produced (Cheirolepidiaceae conifer). Studies on this material are ongoing given the high potential for paleobiological insights.

## Late Triassic Amber Deposits and the Significance of Amber From the Heiligkreuz Fm.

The oldest major outpouring of amber preserved in the fossil record is associated with the CPE, and the greatest volume reported so far comes from the paleosols at Rifugio Dibona section (Roghi et al., 2006a; Seyfullah et al., 2018a). During this climate crisis, increased storm and fire events cause physical damage, so a climate change towards humid conditions were additional stressors that affected the entire terrestrial plant ecosystem triggering an increase in resin production by conifers (Seyfullah et al., 2018b).

Triassic amber is documented in some localities around the world (Seyfullah et al., 2018a) which are restricted roughly to a latitude band between 5°N and 30°N. In Europe the amber coincides well with the various pulsations of the CPE (Figure 13). In Italy, besides the amber from the Heiligkreuz Fm. (e.g., Rifugio Dibona, Heiligkreuz/Santa Croce, Rio

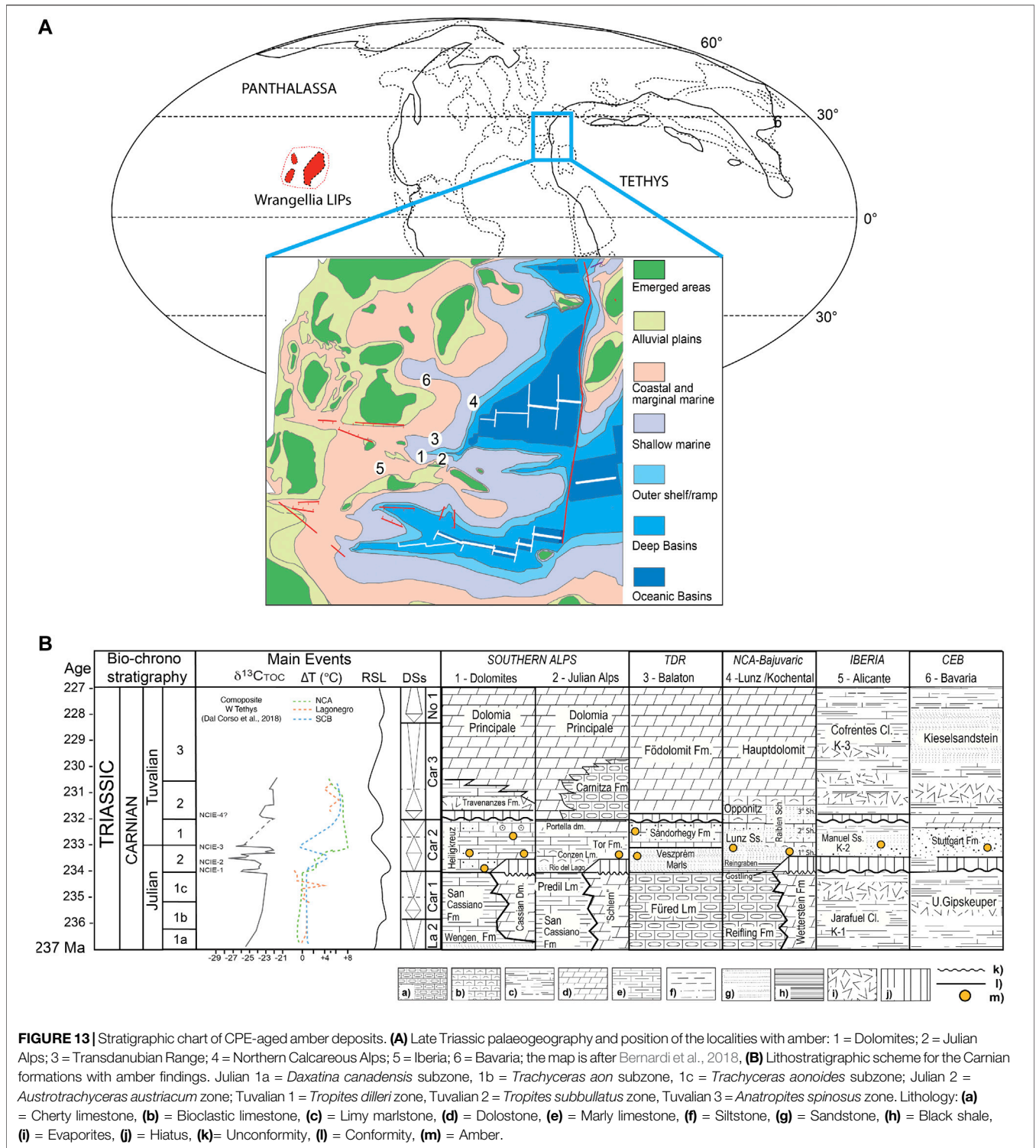


**FIGURE 13** | Stratigraphic chart of CPE-aged amber deposits. **(A)** Late Triassic palaeogeography and position of the localities with amber: 1 = Dolomites; 2 = Julian Alps; 3 = Transdanubian Range; 4 = Northern Calcareous Alps; 5 = Iberia; 6 = Bavaria; the map is after Bernardi et al., 2018. **(B)** Lithostratigraphic scheme for the Carnian formations with amber findings. Julian 1a = *Daxatina canadensis* subzone, 1b = *Trachyceras aon* subzone, 1c = *Trachyceras aonoides* subzone; Julian 2 = *Austrotrachyceras austriacum* zone; Tuvallian 1 = *Tropites dilleri* zone, Tuvallian 2 = *Tropites subbullatus* zone, Tuvallian 3 = *Anatropites spinosus* zone. Lithology: **(a)** = Cherty limestone, **(b)** = Bioclastic limestone, **(c)** = Limy marlstone, **(d)** = Dolostone, **(e)** = Marly limestone, **(f)** = Siltstone, **(g)** = Sandstone, **(h)** = Black shale, **(i)** = Evaporites, **(j)** = Hiatus, **(k)** = Unconformity, **(l)** = Conformity, **(m)** = Amber.

Falzarego, Rif. San Marco, Rifugio Mietres, and Rumerlo sections), amber is also found in the Dogna Valley (Julian Alps) from Tor Fm. (Gianolla et al., 1998a; Preto et al., 2005;

Roghi et al., 2006a), both are Julian in age. Small amounts of Carnian amber have been reported from Austria, from the Lunz Fm. at Lunz (Vávra, 1984; Vávra, 2005; Roghi et al., 2010; Fischer

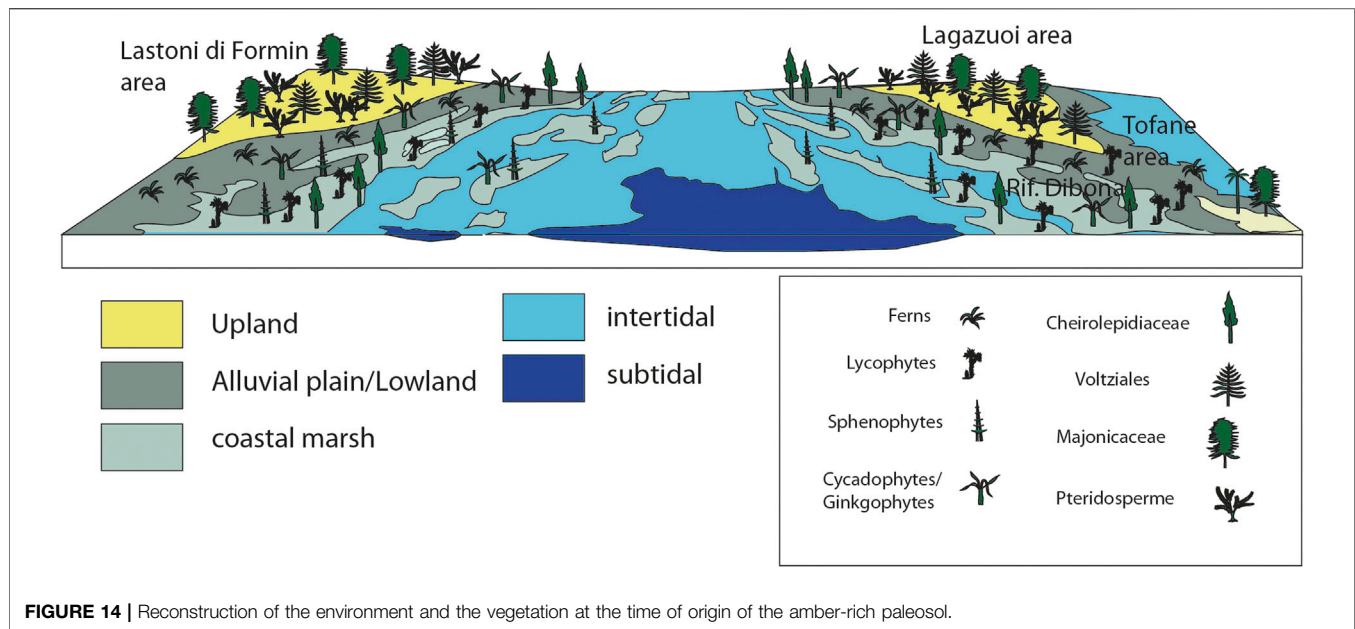


**FIGURE 14** | Reconstruction of the environment and the vegetation at the time of origin of the amber-rich paleosol.

et al., 2017), in the Raibler Schichten in Kochental (Pichler, 1868; Gianolla et al., 1998b) and in the Stuttgart Fm. near Neuwelt (Switzerland) (Figure 13). Kelber and Hansch (1995) figure amber (p. 89, fig. 180) from the Schilfsandstein (Stuttgart Fm.) of northern Bavaria, Germany. In Hungary, a sole piece has been recorded from a drill core of the Barnag Member of the Sándorhegy Fm. and dated to the early Tuvallian (Csillag and Földvári, 2007) while microscopic droplets in palynological slides are reported from the Julian Veszprem Marls and Tuvallian Sándorhegy Formation from the Zsámbék-14 borehole (Baranyi et al., 2018). Spanish (Alicante) Carnian amber (millimetric droplets) has been reported and figured from the Keuper (K2, Manuel Formation) but no further details are known (Peñalver and Delclòs, 2010).

Triassic amber finding outside of Europe do not have a precise dating until now, or do probably not coincide with the time interval of the CPE. For example, the amber found inside seeds in South Africa (Ansorge, 2007), in the Molteno Formation (Karoo Basin) is slightly younger with respect to the CPE; it is probably Tuvallian in age (Langer, 2005), whereas the amber from the Triassic Blue Mesa Member of the Chinle Formation of Arizona (United States) (Litwin and Ash, 1991) is most likely younger, potentially even Norian in age (Seyfullah et al., 2018a). In the Fingal Valley Upper Triassic Coal Measures of the Upper Parmeener Supergroup, Tasmania, small amounts of ambers with very few miniscule inclusions are reported (Stilwell et al., 2020).

Amber in the Dolomites was found throughout the Heiligkreuz Fm. (Preto and Hinnov, 2003; Roghi et al., 2006a; Breda et al., 2009) as early as the first onset of the CPE as included from the base of the Heiligkreuz Fm., within the Borca member, and becoming very abundant in the upper part of the Formation, in the Dibona sandstones. All these findings allow us to be framed

in the two million years that are the time represented by the Heiligkreuz Formation equivalent to the CPE.

## Paleoenvironmental Reconstruction

An attempt is made here for the first time to reconstruct the landscape, environment and vegetation at the time of origin of the paleosols of the Heiligkreuz Fm. based on the sedimentological, palynological and paleobotanical content of the studied horizons. The analysis of the facies and the evolution of the environments show that the area between Lastoni di Formin and Lagazuoi were subjected during the deposition of the Borca Member (Heiligkreuz Fm.) to a progressive infilling of residual basinal areas culminated with a regional flattening recorded by the deposition of loferitic dolostones and marly limestones organized in peritidal cyclothems bounded at the top by karstic dissolution and paleosols (Lithofacies D in Preto and Hinnov, 2003).

The emerged land masses, colonized by plants and animals, were almost entirely flat. The area was characterized by an articulated landscape with sub- and intertidal settings as well as coastal marshes (Figure 14). The areas, characterized today by the important mountain ridges of Lastoni di Formin, Lagazuoi and Tofane, were covered by a mixture of alluvial plain to lowland settings and some areas that were in a more elevated position, although with a very limited vertical extension above the sea level, the so-called up- or hinterland area. The environment was thus a generally wet but also halophytic environment where water was available the entire year long and the plants were adapted to excessive salt (in the water, soil and in the wind) and experienced, thus some physiological drought. The reconstructed paleotopography, based on

geological and sedimentological data, forms the basis of a vegetation type that rarely has been described from coeval settings. It influences deeply also the understanding of the composition of the vegetation covering it.

## The Palynological Climate Signal of the Rifugio Dibona Section

The Rifugio Dibona section is one of the most iconic outcrops for the study of the CPE in a terrestrial/marginal marine setting. Detailed geochemical and sedimentological studies have been carried out (e.g., Gattolin et al., 2013; Dal Corso et al., 2015; Dal Corso et al., 2018) tightly constraining the sedimentological succession corresponding to the CPE.

Additionally, the first studies on Carnian amber and its biological inclusions were carried out (Schmidt et al., 2006; Schmidt et al., 2012; Sidorchuk et al., 2015). Nonetheless, at a first glance the quantitative composition of the macroflora and microflora reported here does not appear to reflect the typical spike in humid elements expected during the CPE. The palynological assemblages are mainly composed of elements from the hinterland and the coastal areas, which are typically xerophytes. However, the lowland elements, living in the environment most sensitive to climate changes, are composed of more abundant hygrophytic than xerophytic elements.

So, does this iconic section exposing the richest amber-bearing paleosol worldwide, constrained by biostratigraphy, geochemistry and sedimentology, in some time not reflect a shift to humid climate? In order to understand the effect of the CPE on the plant communities, the environment and landscape they are living in, as well as the environmental preferences and adaptations of the various plants, has to be taken into account. The landscape reconstructed by the geology and sedimentology is that of a complex coastal and tidal setting. The palynological assemblage is dominated by conifers, which are predominantly considered xerophytic elements. The conifers (e.g., Cheirolepidiaceae, Majonicaceae) had colonized a coastal environment, where water is abundant but not necessarily always available for the plants. Their abundance does, thus, not indicate a drier climate, but rather a xerophytic setting in a local landscape due to a rise in sea water level.

In a larger context, palynological analyses of Carnian (Upper Triassic) successions are well known in the Alpine area from the Dolomites, Carnic Alps, Julian Alps and Northern Calcareous Alps, and the Lunz area, corresponding to the so called northwestern Tethyan margin (Roghi et al., 2010; Mueller et al., 2016b; Dal Corso et al., 2018; Kustatscher et al., 2018). These palynological analyses do provide clear evidence of a shift towards a more humid climatic regime which falls within the framework of the CPE (Dal Corso et al., 2020).

## CONCLUSION

The Heiligkreuz Formation at the Rifugio Dibona is very expanded and crops out over a thickness of 160 m. This section has been studied in detail from a sedimentological and

geochemical view, making it potentially one of the best preserved and continuous sections in the Dolomites. Since the CPE is so well-constrained sedimentologically and geochemically and clearly delimited, it is possible to reconstruct the flora even if the landscape is untypical and the composition of the flora at a first glance would not automatically indicate a humid event. This shows how important it is to keep in consideration also the landscape setting and requirements when studying climate changes. This case study underlines how climate changes influence the floral and faunal composition but cannot completely override the requirements and restrictions of the landscape itself.

On the other hand, it is possible that it is exactly this complex landscape with a high preservation potential in the paleosol horizons that permits to identify the concurrent presence of ancestral (Majonicaceae), Triassic/Mesozoic (Voltziaceae, Cheirolepidiaceae) and modern conifer families (Araucariaceae, Pinaceae and Podocarpaceae) both among the palynomorphs and the macroremains. A high-resolution palynological study in the future will show whether this co-occurrence is restricted to the CPE only, or is part of a general floral turnover or replacement during the Carnian and if the same type of dynamics can be observed also for the fern group.

One of the causes for the simultaneous occurrence of so many different conifer families could be the latitudinal shifts of the biomes due to the four distinct NCIE shifts linked to different LIP volcanic pulses. These would have affected both the precipitation pattern and mean annual temperature (Figure 13) and give origin to migrations fluxes of plants and animals. This theory is supported by the observed immigration pattern of several types of pollen from the high to the low latitudes during the CPE. The extremely dynamic climate and landscape pattern could explain the exceptional mixture of “older” residual and modern conifer families observed in the Rifugio Dibona section. It also would trigger the evolution of the terrestrial and marine plant and animals and increase the origination and speciation rates within the newly developed plant and animal groups (e.g., Dipteridaceae, Bennettitales).

So far the study of the plant fossils is restricted to two main intervals in the Dibona section, the sandstone bank and the paleosols discussed above. The paleosols yielded amber droplets in association with exceptionally preserved isolated leaf fragments and small shoot and cone fragments. This permits not only to integrate the palynomorph assemblage but shows also the high potential of mesofossil collections. However, it raises also the question whether this association of exceptionally preserved dispersed plant mesofossils with amber droplets is a local effect of the landscape or linked to the extent of the volcanic activity during the CPE.

## DATA AVAILABILITY STATEMENT

The original contributions presented in the study are included in the article, further inquiries can be directed to the corresponding author.

## AUTHOR CONTRIBUTIONS

All authors listed have made a substantial, direct, and intellectual contribution to the work and approved it for publication.

## FUNDING

Funds for open access was provided by the University of Vienna.

## REFERENCES

- Ansorge, J. (2007). "Upper Triassic Insects and Amber from Lesotho (South Africa)," in *FossilsX3: Insects, Arthropods, Amber (Abstracts)*. Editor J. Alonso (Spain: Vitoria-Gasteiz), 52–54.
- Balme, B. E. (1995). Fossil *In Situ* Spores and Pollen Grains: an Annotated Catalogue. *Rev. Palaeobot. Palynology* 87, 81–323. doi:10.1016/0034-6667(95)93235-x
- Balme, B. E. (1979). Palynology of Permian-Triassic Boundary Beds at Kap Stosch, East Greenland. *Meddelelser Om. Grønland* 200 (6), 1–37.
- Baranyi, V., Miller, C. S., Ruffell, A., Hounslow, M. W., and Kürschner, W. M. (2018). A Continental Record of the Carnian Pluvial Episode (CPE) from the Mercia Mudstone Group (UK): Palynology and Climatic Implications. *J. Geol. Soc.* 176, 149–166. doi:10.1144/jgs2017-150
- Baranyi, V., Rostási, Á., Raucsik, B., and Kürschner, W. M. (2019). Palynology and Weathering Proxies Reveal Climatic Fluctuations during the Carnian Pluvial Episode (CPE) (Late Triassic) from Marine Successions in the Transdanubian Range (Western Hungary). *Glob. Planet. Change* 177, 157–172. doi:10.1016/j.gloplacha.2019.01.018
- Barrenechea, J. F., López-Gómez, J., and De La Horra, R. (2018). Sedimentology, Clay Mineralogy and Palaeosols of the Mid-carnian Pluvial Episode in Eastern Spain: Insights into Humidity and Sea-Level Variations. *J. Geol. Soc.* 175, 993–1003. doi:10.1144/jgs2018-024
- Barrón, E., Gómez, J. J., Goy, A., and Pieren, A. P. (2006). The Triassic-Jurassic Boundary in Asturias (Northern Spain): Palynological Characterisation and Facies. *Rev. Palaeobot. Palynology* 138, 187–208. doi:10.1016/j.revpalbo.2006.01.002
- Bernardi, M., Gianolla, P., Petti, F. M., Mietto, P., and Benton, M. J. (2018). Dinosaur Diversification Linked with the Carnian Pluvial Episode. *Nat. Commun.* 9, 1499. doi:10.1038/s41467-018-03996-1
- Blomenkemper, P., Kerp, H., Abu Hamad, A., DiMichele, W. A., and Bomfleur, B. (2018). A Hidden Cradle of Plant Evolution in Permian Tropical Lowlands. *Science* 362, 1414–1416. doi:10.1126/science.aau4061
- Bonis, N. R., and Kürschner, W. M. (2012). Vegetation History, Diversity Patterns, and Climate Change across the Triassic/Jurassic Boundary. *Paleobiology* 38, 240–264. doi:10.1666/09071.1
- Bosellini, A., Masetti, D., and Neri, C. (1982). "La geologia del passo del Falzarego," in *Guida alla Geologia del Sudalpino centro-orientale*. Editors A. Castellarin and G. B. Vai (Rome: SOCIETÀ GEOLOGICA ITALIANA), 273–278.
- Bosellini, A. (1984). Progradation Geometries of Carbonate Platforms: Examples from the Triassic of the Dolomites, Northern Italy. *Sedimentology* 31, 1–24. doi:10.1111/j.1365-3091.1984.tb00720.x
- Breda, A., and Preto, N. (2011). Anatomy of an Upper Triassic Continental to Marginal-Marine System: the Mixed Siliciclastic-Carbonate Travenanzes Formation (Dolomites, Northern Italy). *Sedimentology* 58, 1613–1647. doi:10.1111/j.1365-3091.2011.01227.x
- Breda, A., Preto, N., Roghi, G., Furin, S., Meneguolo, R., Ragazzi, E., et al. (2009). The Carnian Pluvial Event in the Tofane Area (Cortina d'Ampezzo, Dolomites, Italy). *Geo. Alp.* 6, 80–115.
- Buratti, N., and Cirilli, S. (2007). Microfloristic Provincialism in the Upper Triassic Circum-Mediterranean Area and Palaeogeographic Implication. *Gebios* 40, 133–142. doi:10.1016/j.gebios.2006.06.003

## ACKNOWLEDGMENTS

We warmly thank Paolo Fedele (Cortina d'Ampezzo) for his enthusiasm and sharing his findings with us. We would wish to thank Miriam A. Slodownik (Göttingen) for preparing amber droplets for microscopic analysis and for detecting plant fossils in the palaeosol samples, and Laura Skadell (Göttingen) for screening numerous amber droplets for inclusions. The reviewers Daoliang Chu (Wuhan) and Grzegorz Pacyna (Kraków) are thanked for their helpful and constructive remarks.

- Césari, S. N., and Colombi, C. E. (2013). A New Late Triassic Phytogeographical Scenario in Westernmost Gondwana. *Nat. Commun.* 4, 1889. doi:10.1038/ncomms2917
- Clement-Westerhof, J. A. (1987). Aspects of Permian Palaeobotany and Palynology, VII. The Majonicaceae, a New Family of Late Permian Conifers. *Rev. Palaeobot. Palynology* 52, 375–402. doi:10.1016/0034-6667(87)90066-2
- Clement-Westerhof, J. A. (1974). *In Situ* pollen from Gymnospermous Cones from the Upper Permian of the Italian Alps - A Preliminary Account. *Rev. Palaeobot. Palynology* 17, 63–73. doi:10.1016/0034-6667(74)90092-X
- Colombi, C., Martínez, R. N., Césari, S. N., Alcober, O., Limarino, C. O., and Montañez, I. (2021). A High-Precision U-Pb Zircon Age Constrains the Timing of the Faunistic and Palynofloristic Events of the Carnian Ischigualasto Formation, San Juan, Argentina. *J. S. Am. Earth Sci.* 111, 103433. doi:10.1016/j.jsames.2021.103433
- Csillag, G., and Földvári, M. (2007). "Upper Triassic Amber Fragments from the Balaton Highlands, Hungary," in *Annual Report of the Geological Institute of Hungary 2005* (Budapest: Geological Institute of Hungary), 37–46. [in Hungarian].
- Dal Corso, J., Bernardi, M., Sun, Y., Song, H., Seyfullah, L. J., Preto, N., et al. (2020). Extinction and Dawn of the Modern World in the Carnian (Late Triassic). *Sci. Adv.* 6, eaba0099. doi:10.1126/sciadv.aba0099
- Dal Corso, J., Gianolla, P., Newton, R. J., Franceschi, M., Roghi, G., Caggiati, M., et al. (2015). Carbon Isotope Records Reveal Synchronicity between Carbon Cycle Perturbation and the "Carnian Pluvial Event" in the Tethys Realm (Late Triassic). *Glob. Planet. Change* 127, 79–90. doi:10.1016/j.gloplacha.2015.01.013
- Dal Corso, J., Gianolla, P., Rigo, M., Franceschi, M., Roghi, G., Mietto, P., et al. (2018). Multiple Negative Carbon-Isotope Excursions during the Carnian Pluvial Episode (Late Triassic). *Earth-Science Rev.* 185, 732–750. doi:10.1016/j.earscirev.2018.07.004
- Dal Corso, J., Mietto, P., Newton, R. J., Pancost, R. D., Preto, N., Roghi, G., et al. (2012). Discovery of a Major Negative  $^{13}\text{C}$  Spike in the Carnian (Late Triassic) Linked to the Eruption of Wrangellia Flood Basalts. *Geology* 40, 79–82. doi:10.1130/g32473.1
- Dal Corso, J., Preto, N., Kustatscher, E., Mietto, P., Roghi, G., and Jenkyns, H. C. (2011). Carbon-isotope Variability of Triassic Amber, as Compared with Wood and Leaves (Southern Alps, Italy). *Palaeogeogr. Palaeoclimatol. Palaeoecol.* 302, 187–193. doi:10.1016/j.palaeo.2011.01.007
- Dal Corso, J., Song, H. J., Callegaro, S., Chu, D. L., Sun, Y. D., Hilton, J., et al. (2022). Environmental Crises at the Permian-Triassic Mass Extinction. *Nat. Rev. Earth Environ.* doi:10.1038/s43017-021-00259-4
- De Zanche, V., Gianolla, P., Mietto, P., Siorpaes, C., and Vail, P. R. (1993). Triassic Sequence Stratigraphy in the Dolomites (Italy). *Mem. Sci. Geol.* 45, 1–27.
- De Zanche, V., Gianolla, P., and Roghi, G. (2000). Carnian stratigraphy in the Raibl/Cave del Predil area (Julian Alps, Italy). *Ecl. Geol. Helv.* 93, 331–347.
- DiMichele, W., Mamay, S., Chaney, D., Hook, R., and Nelson, W. (2001). An Early Permian Flora with Late Permian and Mesozoic Affinities From North-Central Texas. *J. Paleontol.* 75 (2), 449–460. doi:10.1666/0022-3360(2001)0752.0.CO;2
- Dolby, J. H., and Balme, B. E. (1976). Triassic Palynology of the Carnarvon Basin, Western Australia. *Rev. Palaeobot. Palynology* 22, 105–168. doi:10.1016/0034-6667(76)90053-1
- Fischer, T. C., Sonibare, O. O., Aschauer, B., Kleine-Benne, E., Braun, P., and Meller, B. (2017). Amber from the Alpine Triassic of Lunz (Carnian, Austria): a Classic Palaeobotanical Site. *Palaeontol.* 60, 743–759. doi:10.1111/pala.12313

- Forste, G., Kustatscher, E., Ragazzi, E., and Roghi, G. (2022). Amber Droplets in the Southern Alps (NE Italy): a Link between Their Occurrences and Main Humid Episodes in the Triassic. *Riv. It. Paleontol. Strat.* 128, 69–79. doi:10.54103/2039-4942/15381
- Forste, G., Kustatscher, E., Van Konijnenburg-van Cittert, J. H. A., Looy, C. V., and Kerp, H. (2017). Conifer Diversity in the Kungurians of Europe—Evidence from Dwarf-Shoot Morphology. *Rev. Palaeobot. Palynology* 244, 308–315. doi:10.1016/j.revpalbo.2017.01.004
- Franz, M., Nowak, K., Berner, U., Heunisch, C., Bandel, K., Röhling, H.-G., et al. (2014). Eustatic Control on Epicontinental Basins: The Example of the Stuttgart Formation in the Central European Basin (Middle Keuper, Late Triassic). *Glob. Planet. Change* 122, 305–329. doi:10.1016/j.gloplacha.2014.07.010
- Gattolin, G., Breda, A., and Preto, N. (2013). Demise of Late Triassic Carbonate Platforms Triggered the Onset of a Tide-Dominated Depositional System in the Dolomites, Northern Italy. *Sediment. Geol.* 297, 38–49. doi:10.1016/j.sedgeo.2013.09.005
- Gattolin, G., Preto, N., Breda, A., Franceschi, M., Isotton, M., and Gianolla, P. (2015). Sequence Stratigraphy After the Demise of a High-Relief Carbonate Platform (Carnian of the Dolomites): Sea-Level and Climate Disentangled. *Palaeogeogr. Palaeoclimatol. Palaeoecol.* 423, 1–17.
- Gianolla, P., De Zanche, V., and Mietto, P. (1998b). “Triassic Sequence Stratigraphy in the Southern Alps (Northern Italy): Definition of Sequences and Basin Evolution,” in *Mesozoic and Cenozoic Sequence Stratigraphy of European Basin* (Tulsa/Oklahoma: SEPM Special Publication), 719–747.
- Gianolla, P., De Zanche, V., and Roghi, G. (2003). An Upper Tuvallian (Triassic) Platform-Basin System in the Julian Alps: the Start-Up of the Dolomia Principale (Southern Alps, Italy). *Facies* 49, 135–150. doi:10.1007/s10347-003-0029-7
- Gianolla, P., Morelli, C., Cucato, M., and Siorpaes, C. (2018). Note Illustrative della Carta Geologica d'Italia alla scala 1:50.000, Foglio 016, Dobbiaco, ISPRA, 2018, Carta. *Systemcart*, 1–283.
- Gianolla, P., Roghi, G., and Ragazzi, E. (1998a). Upper Triassic Amber in the Dolomites (Northern Italy). A Paleoclimatic Indicator? *Riv. It. Paleontol. Strat.* 104, 381–390.
- Grauvogel-Stamm, L. (1978). *La flore du Grès à Voltzia (Buntsandstein supérieur) des Vosges du Nord (France). Morphologie, anatomie, interprétations phylogénique et paléogéographique (= Université Louis Pasteur de Strasbourg.* Strasbourg: Université Louis Pasteur
- Grauvogel-Stamm, L., and Düringer, P. (1983). Annalepis zeilleri Fliche 1910 emend., un organe reproducteur de Lycophyte de la Lettenkohle de l'Est de la France. Morphologie, spores in situ et paléocologie. *Geologische Rundschau* 72, 23–51.
- Helby, R. J., and Martin, A. R. H. (1965). Cyclostrobus gen. nov., Cones of Lycopsidean Plants from the Narrabeen Group (Triassic) of New South Wales. *Aust. J. Botany* 13, 389–404.
- Keim, L., and Brandner, R. (2001). Facies Interfingering and Synsedimentary Tectonics on Late Ladinian-Early Carnian Carbonate Platforms (Dolomites, Italy). *Int. J. Earth Sci.* 90, 813–830. doi:10.1007/s005310000192
- Keim, L., Brandner, R., Krystyn, L., and Mette, W. (2001). Termination of Carbonate Slope Progradation: an Example from the Carnian of the Dolomites, Northern Italy. *Sediment. Geol.* 143, 303–323. doi:10.1016/S0037-0738(01)00106-3
- Kelber, K.-P., and Hansch, W. (1995). Keuperpflanzen. Die Enträtselung einer über 200 Millionen Jahre alten Flora. *Museo* 11, 1–157.
- Kelber, K.-P., and Van Konijnenburg-Van Cittert, J. H. A. (1998). Equisetites arenaceus from the Upper Triassic of Germany with Evidence for Reproductive Strategies. *Rev. Palaeobot. Palynol.* 100, 1–6.
- Kustatscher, E., Ash, S. R., Karasev, E., Pott, C., Vajda, V., Yu, J., et al. (2018). “Flora of the Late Triassic,” in *The Late Triassic World*. Editor L. H. Tanner (Cham: Springer), Vol. 46, 545–622. Topics in Geobiology. doi:10.1007/978-3-319-68009-5\_13
- Kustatscher, E., Bizzarrini, F., and Roghi, G. (2011). Plant Fossils in the Cassian Beds and Other Carnian Formations of the Southern Alps (Italy). *Geo. Alp.* 8, 146–155.
- Kustatscher, E., Michael, W., and Van Konijnenburg-Van Cittert, J. H. A. (2010). Lycophytes from the Middle Triassic (Anisian) Locality Kühwiesenkopf (Monte Prà della Vacca) in the Dolomites (Northern Italy). *Palaeontology* 53, 595–626. doi:10.1111/j.1475-4983.2010.00948.x
- Kustatscher, E., Nowak, H., Forste, G., Roghi, G., and Van Konijnenburg-Van Cittert, J. H. A. (2019). Triassic Macro- and Microfloras of the Eastern Southern Alps. *Geo. Alp.* 16, 5–43.
- Labandeira, C. C. (2006). The Four Phases of Plant-Arthropod Associations in Deep Time. *Geol. Acta* 4, 409–438.
- Langer, M. C. (2005). Studies on Continental Late Triassic Tetrapod Biochronology. II. The Ischigualastian and a Carnian Global Correlation. *J. South Am. Earth Sci.* 19, 219–239
- Litwin, R. J., and Ash, S. R. (1991). First Early Mesozoic Amber in the Western Hemisphere. *Geol.* 19, 273–276. doi:10.1130/0091-7613(1991)019<0273:femait>2.3.co;2
- Looy, C. V., Twitchett, R. J., Dilcher, D. L., Van Konijnenburg-Van Cittert, J. H., and Visscher, H. (2001). Life in the End-Permian Dead Zone. *Proc. Natl. Acad. Sci. U.S.A.* 98 (14), 7879–7883. doi:10.1073/pnas.131218098
- Lu, J., Zhang, P., Dal Corso, J., Yang, M., Wignall, P. B., Greene, S. E., et al. (2021). Volcanically Driven Lacustrine Ecosystem Changes during the Carnian Pluvial Episode (Late Triassic). *Proc. Natl. Acad. Sci. U.S.A.* 118 (40), e2109895118. doi:10.1073/pnas.2109895118
- Maron, M., Muttoni, G., Dekkers, M. J., Mazza, M., Roghi, G., Breda, A., et al. (2017). Contribution to the Magnetostratigraphy of the Carnian: New Magneto-Biostratigraphic Constraints from Pignola-2 and Dibona Marine Sections, Italy. *nos* 50, 187–203. doi:10.1127/nos/2017/0291
- Mazaheri-Johari, M., Gianolla, P., Mather, T. A., Frieling, J., Chu, D., and Dal Corso, J. (2021). Mercury Deposition in Western Tethys during the Carnian Pluvial Episode (Late Triassic). *Sci. Rep.* 11, 17339. doi:10.1038/s41598-021-96890-8
- Miller, C. S., Peterse, F., da Silva, A.-C., Baranyi, V., Reichart, G. J., and Kürschner, W. M. (2017). Astronomical Age Constraints and Extinction Mechanisms of the Late Triassic Carnian Crisis. *Sci. Rep.* 7, 2557. doi:10.1038/s41598-017-02817-7
- Mueller, S., Hounslow, M. W., and Kürschner, W. M. (2016a). Integrated Stratigraphy and Palaeoclimate History of the Carnian Pluvial Event in the Boreal Realm; New Data from the Upper Triassic Kapp Toscana Group in Central Spitsbergen (Norway). *J. Geol. Soc.* 173, 186–202. doi:10.1144/jgs2015-028
- Mueller, S., Krystyn, L., and Kürschner, W. M. (2016b). Climate Variability during the Carnian Pluvial Phase - A Quantitative Palynological Study of the Carnian Sedimentary Succession at Lunz Am See, Northern Calcareous Alps, Austria. *Palaeogeogr. Palaeoclimatol. Palaeoecol.* 441, 198–211. doi:10.1016/j.palaeo.2015.06.008
- Neri, C., Gianolla, P., Furlanis, S., Caputo, R., and Bosellini, A. (2007). *Carta Geologica d'Italia Alla Scala 1:50000, Foglio 29 Cortina d'Ampezzo, and Note Illustrative*. Roma: APAT, 200.
- Nowak, H., Schneebeli-Hermann, E., and Kustatscher, E. (2018). Correlation of Lopingian to Middle Triassic Palynozones. *J. Earth Sci.* 29, 755–777. doi:10.1007/s12583-018-0790-8
- Pacyna, G., Barbacka, M., Zdebska, D., Ziaja, J., Fijałkowska-Mader, A., Bóka, K., et al. (2017). A New Conifer from the Upper Triassic of Southern Poland Linking the Advanced Voltzian Type of Ovuliferous Scale with *Brachyphyllum* - *Pagiophyllum* -like Leaves. *Rev. Palaeobot. Palynology* 245, 28–54. doi:10.1016/j.revpalbo.2017.05.015
- Peñalver, E., and Delclòs, X. (2010). “Spanish Amber,” in *Biodiversity of Fossils in Amber from the Major World Deposits*. Editor D. Penney (Manchester, UK: Siri Scientific Press), 236–270.
- Pichler, A. (1868). Beiträge zur Geognosie Tirols. XI. Fossiles Harz. *J. K.-k. Geol. Reich.* 18, 45–52.
- Preto, N., and Hinnov, L. A. (2003). Unraveling the Origin of Carbonate Platform Cyclothem in the Upper Triassic Durrenstein Formation (Dolomites, Italy). *J. Sediment. Res.* 73, 774–789. doi:10.1306/030503730774
- Preto, N., Kustatscher, E., and Wignall, P. B. (2010). Triassic Climates - State of the Art and Perspectives. *Palaeogeogr. Palaeoclimatol. Palaeoecol.* 290, 1–10. doi:10.1016/j.palaeo.2010.03.015
- Preto, N., Roghi, G., and Gianolla, P. (2005). Carnian Stratigraphy of the Dognà Area (Julian Alps, Northern Italy): Tessera of a Complex Palaeogeography. *Boll. Soc. Geol. It.* 124, 269–279.

- Retallack, G. J., Veevers, J. J., and Morante, R. (1996). Global Coal Gap between Permian-Triassic Extinction and Middle Triassic Recovery of Peat-Forming Plants. *Geol. Soc. Am. Bull.* 108, 195–207. doi:10.1130/0016-7606(1996)108<0195:gcbpt>2.3.co;2
- Rigo, M., Preto, N., Roghi, G., Tateo, F., and Mietto, P. (2007). A Rise in the Carbonate Compensation Depth of Western Tethys in the Carnian (Late Triassic): Deep-Water Evidence for the Carnian Pluvial Event. *Palaeogeogr. Palaeoclimatol. Palaeoecol.* 246, 188–205. doi:10.1016/j.palaeo.2006.09.013
- Roghi, G., Gianolla, P., Minarelli, L., Pilati, C., and Preto, N. (2010). Palynological Correlation of Carnian Humid Pulses throughout Western Tethys. *Palaeogeogr. Palaeoclimatol. Palaeoecol.* 290, 89–106. doi:10.1016/j.palaeo.2009.11.006
- Roghi, G., Kustatscher, E., Ragazzi, E., and Giusberti, L. (2017). Middle Triassic Amber Associated with Voltzialean Conifers from the Southern Alps of Italy. *Riv. It. Paleontol. Strat.* 123, 193–202.
- Roghi, G., Kustatscher, E., and van Konijnenburg-van Cittert, J. H. A. (2006b). Late Triassic Plants from Julian Alps (Italy). *Boll. Soc. Paleont. It.* 45, 133–140.
- Roghi, G. (2004). Palynological investigations in the Carnian of the Cave del Predil area (Julian Alps, NE Italy). *Rev. Palaeobot. Palynology* 132, 1–35. doi:10.1016/j.revpalbo.2004.03.001
- Roghi, G., Ragazzi, E., and Gianolla, P. (2006a). Triassic Amber of the Southern Alps (Italy). *Palaios* 21, 143–154. doi:10.2110/palo.2005.p05-68
- Rothwell, G. W., Mapes, G., Stockey, R. A., and Hilton, J. (2012). The Seed Cone *Eathiestrobus* Gen. nov.: Fossil Evidence for a Jurassic Origin of Pinaceae. *Am. J. Bot.* 99, 708–720. doi:10.3732/ajb.1100595
- Ruffell, A., Simms, M. J., and Wignall, P. B. (2016). The Carnian Humid Episode of the Late Triassic: A Review. *Geol. Mag.* 153, 271–284. doi:10.1017/S0016756815000424
- Russo, F., Neri, C., Mastandrea, A., and Laghi, G. (1991). Depositional and diagenetic history of the Alpe di Specie (Seelandalpe) fauna (Carnian, northeastern Dolomites). *Facies* 25, 187–210. doi:10.1007/bf02536759
- Sadowski, E.-M., Schmidt, A. R., Seyfullah, L. J., Solórzano-Kraemer, M. M., Neumann, C., Perrichot, V., et al. (2021). Conservation, Preparation and Imaging of Diverse Ambers and Their Inclusions. *Earth-Sc. Rev.* 220, 103653. doi:10.1016/j.earscirev.2021.103653
- Scherer, M. (1977). Preservation, Alteration and Multiple Cementation of Aragonitic Skeletons from the Cassian Beds (U. Triassic, Southern Alps): Petrographic and Geochemical Evidence. *Neues Jb. Geol. Paläontol. Abh.* 154, 213–262.
- Schmidt, A. R., Jancke, S., Lindquist, E. E., Ragazzi, E., Roghi, G., Nascimbene, P. C., et al. (2012). Arthropods in Amber from the Triassic Period. *Proc. Natl. Acad. Sci. U.S.A.* 109, 14796–14801. doi:10.1073/pnas.1208464109
- Schmidt, A. R., Ragazzi, E., Coppellotti, O., and Roghi, G. (2006). A Microworld in Triassic Amber. *Nature* 444, 835. doi:10.1038/444835a
- Senowbari-Daryan, B., Flügel, E., and Preto, N. (2001). *Tethysocarnia Cautica* N. Gen. N. sp., a Sessile Foraminifer from Late Ladinian and Carnian Reefs of the Western and Southern Tethys. *Geol. Paleontol.* 35, 105–119.
- Seyfullah, L. J., Beimforde, C., Dal Corso, J., Perrichot, V., Rikkinen, J., and Schmidt, A. R. (2018b). Production and Preservation of Resins - Past and Present. *Biol. Rev.* 93, 1684–1714. doi:10.1111/brv.12414
- Seyfullah, L. J., Roghi, G., Corso, J. D., and Schmidt, A. R. (2018a). The Carnian Pluvial Episode and the First Global Appearance of Amber. *J. Geol. Soc.* 175, 1012–1018. doi:10.1144/jgs2017-143
- Sidorchuk, E. A., Schmidt, A. R., Ragazzi, E., Roghi, G., and Lindquist, E. E. (2015). Plant-feeding Mite Diversity in Triassic Amber (Acari: Tetrápodili). *J. Syst. Palaeontol.* 13, 129–151. doi:10.1080/14772019.2013.867373
- Simms, M. J., and Ruffell, A. H. (1990). Climatic and Biotic Change in the Late Triassic. *J. Geol. Soc.* 147, 321–327. doi:10.1144/gsjgs.147.2.0321
- Simms, M. J., Ruffell, A. H., and Johnson, L. A. (1995). “Biotic and Climatic Changes in the Carnian (Triassic) of Europe and Adjacent Areas,” in *The Shadow of the Dinosaurs: Early Mesozoic Tetrapods*. Editors N.C. Fraser and H. D. Sues (Cambridge: Cambridge University Press), 352–365.
- Simms, M. J., and Ruffell, A. H. (1989). Synchronicity of Climatic Change and Extinctions in the Late Triassic. *Geol.* 17, 265–268. doi:10.1130/0091-7613(1989)017<0265:soccae>2.3.co;2
- Stanley, G. D., Jr. (2003). The Evolution of Modern Corals and Their Early History. *Earth-Science Rev.* 60, 195–225. doi:10.1016/s0012-8252(02)00104-6
- Stefani, M., Furin, S., and Gianolla, P. (2010). The Changing Climate Framework and Depositional Dynamics of Triassic Carbonate Platforms from the Dolomites. *Palaeogeogr. Palaeoclimatol. Palaeoecol.* 290, 43–57. doi:10.1016/j.palaeo.2010.02.018
- Stilwell, J. D., Langendam, A., Mays, C., Sutherland, L. J. M., Arillo, A., Bickel, D. J., et al. (2020). Amber from the Triassic to Paleogene of Australia and New Zealand as Exceptional Preservation of Poorly Known Terrestrial Ecosystems. *Sci. Rep.* 10, 5703. doi:10.1038/s41598-020-62252-z
- Sun, Y. D., Wignall, P. B., Joachimski, M. M., Bond, D. P. G., Grasby, S. E., Lai, X. L., et al. (2016). Climate Warming, Euxinia and Carbon Isotope Perturbations during the Carnian (Triassic) Crisis in South China. *Earth Planet. Sci. Lett.* 444, 88–100. doi:10.1016/j.epsl.2016.03.037
- Tanner, L. H. (2018). “Climates of the Late Triassic: Perspectives, Proxies and Problems,” in *The Late Triassic World*. Editor L. H. Tanner (Cham: Springer), 59–90. Topics in Geobiology 46. doi:10.1007/978-3-319-68009-5\_3
- Tomimatsu, Y., Nozaki, T., Sato, H., Takaya, Y., Kimura, J. I., Chang, Q., et al. (2020). Marine Osmium Isotope Record during the Carnian “Pluvial Episode” (Late Triassic) in the Pelagic Panthalassa Ocean. *Glob. Planet. Ch.* 197, 103387. doi:10.1016/j.gloplacha.2020.103387
- Utting, J. (2004). Reworked Miospores in the Upper Paleozoic and Lower Triassic of the Northern Circum-Polar Area and Selected Localities. *Palynology* 28, 75–119. doi:10.2113/28.1.75
- Vávra, N. (2005). Bernstein und verwandte Organische Minerale aus Österreich. *Beitr. Paläont.* 29, 255280.
- Vávra, N. (1984). Reich an armen Fundstellen: Übersicht über die fossilen Harze Österreichs. *Stuttg. Beiträge zur Naturkd. Ser. C* 18, 9–14.
- Zhang, J., Lenz, O. K., Wang, P., and Hornung, J. (2021). The Eco-Plant Model and its Implication on Mesozoic Dispersed Sporomorphs for Bryophytes, Pteridophytes, and Gymnosperms. *Rev. Palaeobot. Palynology* 293, 104503. doi:10.1016/j.revpalbo.2021.104503
- Zhang, Y., Li, M., Ogg, J. G., Montgomery, P., Huang, C., Chen, Z.-Q., et al. (2015). Cycle-calibrated Magnetostratigraphy of Middle Carnian from South China: Implications for Late Triassic Time Scale and Termination of the Yangtze Platform. *Palaeogeogr. Palaeoclimatol. Palaeoecol.* 436, 135–166. doi:10.1016/j.palaeo.2015.05.033

**Conflict of Interest:** The authors declare that the research was conducted in the absence of any commercial or financial relationships that could be construed as a potential conflict of interest.

**Publisher’s Note:** All claims expressed in this article are solely those of the authors and do not necessarily represent those of their affiliated organizations, or those of the publisher, the editors and the reviewers. Any product that may be evaluated in this article, or claim that may be made by its manufacturer, is not guaranteed or endorsed by the publisher.

Copyright © 2022 Roghi, Gianolla, Kustatscher, Schmidt and Seyfullah. This is an open-access article distributed under the terms of the Creative Commons Attribution License (CC BY). The use, distribution or reproduction in other forums is permitted, provided the original author(s) and the copyright owner(s) are credited and that the original publication in this journal is cited, in accordance with accepted academic practice. No use, distribution or reproduction is permitted which does not comply with these terms.